Effect of medium properties of fermentation broths on the oxygen mass transfer in bubble columns

L.M.L. Crasborn

A thesis presented for the degree of Bachelor of Science
at the Delft University of Technology,
to be defended on Wednesday November 10, 2021 at 14:30.

Student number:	4656644	
Project duration:	August 17, 2021 – November 10, 2021	
Thesis committee:	PhD Candidate L Puiman	Daily supervisor
	PhD Candidate M.P. Elisiário	Daily supervisor
	DR. Ir. C. Haringa,	Supervisor
	Dr. A.J.J. Straathof	

TU Delft Delft University of Technology

***Abstract*— Syngas fermentation is a promising novel method for production ethanol, which can be turned into biofuels. The oxygen mass transfer from the gas to the liquid phase is often the bottleneck in these processes. To overcome this, it is important to know what factors impact this mass transfer. In this research, the impact of syngas fermentation broths and ethanol, one of the main products of these processes, is determined. This is done by evaluating the specific area (a), mass transfer rate (k_L) and the volumetric mass transfer rate (k_La), as an effect of medium properties in a small diameter bubble column. An increase in the specific area and k_La and a decrease in the k_L was found for all media with added ethanol compared to those without ethanol. A negative correlation was found between the biomass concentration and the k_L. The presence of surface active compounds led to a decrease in mean bubble diameter and an increase in the gas holdup and specific surface area in the column.**

I. Introduction

The current climate crisis leads to a rising demand for sustainable energy sources. Biofuels are a promising branch of these developments (Naik et al., 2010). A novel way method for the production of biofuels is the syngas fermentation process. Syngas is produced by the gasification of carbonaceous compounds like solid waste, biomass or solid fuels. It is also a byproduct of the fossil fuel industry. By using biological conversion, syngas can be converted into useful products. One of these products is ethanol, this can be converted to biofuels and bioplastics (Abubackar et al., 2011).

For these processes to work efficiently, the cells need enough substrate to grow and produce ethanol. Whereas the syngas inflow is easily adjusted, one also needs to take the rate that the gasses diffuse into the medium into account. This mass transfer rate is often the bottleneck in fermentation processes (Naik et al., 2010). It is described by the volumetric mass transfer coefficient (k_La), which consists of two terms. The liquid side mass transfer coefficient (k_L) is the rate at which mass diffuses into the liquid phase [1]. The specific volume, which is obtained by dividing the total gas-liquid surface area (m^2) by the total liquid volume, is expressed as a (m^{-1}) (Straathof & Heijnen, 2020). By understanding what factors influence the mass transfer in these processes, a higher yield can possibly be obtained in these processes. Despite the vast amount of research that has been done in this area, a lot of these factors are still unknown (Besagni et al. (2016); Galaction et al. (2004)). Especially the effect of fermentation broth is not understood at the level that it needs to be to accurately predict the mass transfer coefficient. To explore this effect in dept, it is useful to determine the effect of several medium properties on the specific surface area, the mass transfer coefficient and the volumetric mass transfer coefficient. First, the key concepts for this research will be defined.

Flow regimes

The k_La is largely dependent on the total area of the bubbles in the column. A bubble column has different types of flow regimes, which are highly dependent on the superficial gas velocity and the column diameter (Ruzicka et al., 2003). Three main regimes are identified; the homogeneous, heterogeneous and transition flow regime. At low superficial gas velocities, the homogeneous regime takes place. Bubbles are uniformly sized and follow a relatively straight vertical path to the top op the liquid. Coalescence and bubble breakup occur seldom, leading to small bubble size distributions.The heterogeneous flow regime is instated at higher superficial gas velocities and is characterised by bigger bubbles that vary a lot in size. The bubbles don't follow a straight path to the top but swirl trough the liquid. The transition flow regime operates between these two regimes and has properties of both (Shaikh & Al-Dahhan, 2007). The choice of flow regime for the experiment has a lot of influence on the surface area and thus the k_La. In this research, the experiments will be conducted in the homogeneous regime as this leads to a higher k_La (Kantarci et al., 2005).

Surface tension

Surface tension mostly affects the bubble size in the column. As the surface tension decreases, the bubble size decreases. This happens because of the inhibition of bubble coalescence and enhancement of bubble breakup (Eastoe & Dalton, 2000). This stabilises the homogeneous flow regime and increases the gas holdup, leading to a larger gas-liquid surface area (Yan et al., 2020). This effect is caused by surfactants that adhere to the gas-liquid interface. They stabilise the bubble surface by forming ionic bonds with water and each other (Kim et al., 2017). However, this presence at the gas-liquid surface area also inhibits mass transfer from the bubbles to the liquid phase, which lowers the k_L (Huang & Saito, 2017). Surface tension is a dynamic parameter, meaning that it can change over time. In solutions with surface active compounds (surfactants), it will change with the migration of surfactants to the bubble interface. The equilibrium value for the surface tension is reached when the surface is fully satisfied with surfactants (Eastoe & Dalton, 2000).

Viscosity

The effect of viscosity on the mass transfer is dependent on how viscous the medium is. At low values, it is reported to increase gas holdup and stabilise a homogeneous regime (Ruzicka et al., 2003). At higher values, it decreases gas holdup (Figure 1) and promotes a heterogeneous regime (Zahradnik et al., 1987). With increasing viscosity, the k_La decreases (Figure 2). This is due to a higher rate of bubble coalescence, perturbation of bubble dispersion, a lower bubble rising velocity and reduction of turbulence. This leads to a decrease of interfacial area and a decrease in the amount of fresh medium that comes into contact with a bubble (Thobie et al., 2017).

Ethanol

Ethanol is one of the main products of syngas fermentation and thus an interesting component to study in fermentation

[1] It is assumed that k_g, the gas side of this coefficient can be neglected in respect to the liquid mass transfer coefficient.

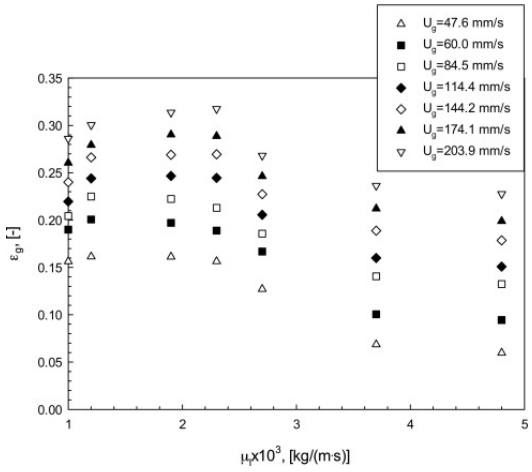

Fig. 1: Effect of the viscosity on the gas holdup (Kim et al., 2017)

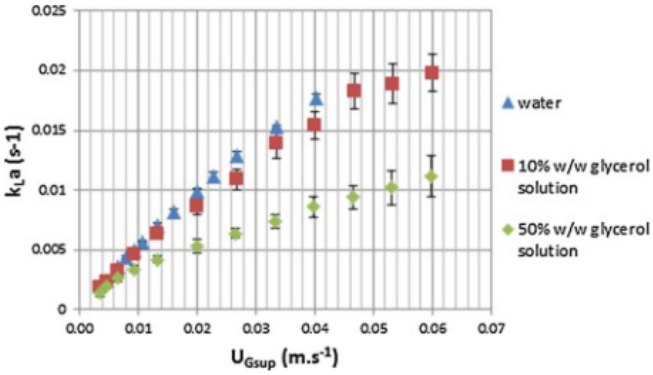

Fig. 2: The evolution of the k_La with the superficial gas velocity for three liquid phases with different increasing levels of viscosity from water to 50% w/w glycerol (Thobie et al., 2017).

broths (Sun et al., 2019). Previous research showed that adding ethanol to water significantly improves the volumetric mass transfer coefficient (k_La) (Jamialahmadi and Müller-Steinhagen (1992); Besagni et al. (2016); Wagenaar (2021); Öztürk et al. (1987)). This happens because ethanol acts as a surfactant which decreases the surface tension, this causes a decrease in bubble size. Furthermore, it decreases the occurrence of coalescence by stabilizing the liquid between two gas bubbles which leads to a bigger interfacial area between the gas and liquid phase (Jamialahmadi & Müller-Steinhagen, 1992). It also increases the gas holdup and decreases the superficial velocity of the bubbles.

It has been shown that the addition of ethanol increases the k_La until a plateau is reached (Table I: from a certain ethanol concentration (around 2%w/w) there is no additional increase in mass transfer rate observed.

At this concentration, the whole surface is satisfied with ethanol, this is called the critical micelle concentration (CMC). Ethanol that is added after that will localize in the bulk where it will have less influence on the mass transfer

TABLE I: Ethanol concentrations where a plateau in the k_La is reached in various research.

Reactor configuration	Plateau ethanol concentration (%w/w)	Source
Stirred tank reactor	2.5	Wagenaar (2021)
Bubble column reactor	1 - 2.5	Besagni et al. (2016)
Bubble column reactor	2.5	Jia et al. (2014)

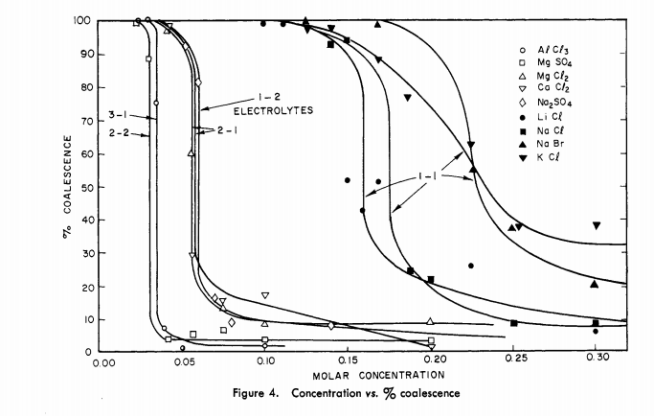

Fig. 3: The relation between the molar concentration of salts and the percentage of bubble coalescence for various salts Lessard and Zieminski, 1971.

coefficient (Kluytmans et al., 2003). The concentration where this happens varies between different studies, as can be seen in Table I.

Minerals

In general, when salts are added to the medium, the k_La increases (Godbole et al., 1983). This happens because minerals prevent bubble coalescence by increasing the surface tension (Figure 3, this increase in the interfacial area (Lessard & Zieminski, 1971). The effect of salts on the k_L is less clear Pegram and Record (2007) reports a negative effect on the k_L due to salt ions that adhere to the gas-liquid interface and thus block the transfer of oxygen. Godbole et al. (1983) report a positive effect on the k_L, which is explained by the "shuttle effect". Alper et al. (1980) and Alper and Öztürk (1986) described this effect. Particles at the gas-liquid interface can absorb oxygen and desorb it in the bulk liquid. This leads to a decrease in the mass transfer rate. These particles also cause extra turbulence at the gas-liquid interface and thus a bigger supply of fresh medium (Kluytmans et al., 2003). The surface tension is increased by salts because they dissolve into ions. The ions attract the polar water molecules and thus create a stable liquid layer (Weissenborn & Pugh, 1995). According to Henry and Craig (2010), coalescence is only inhibited by salts where both ions are attracted or repelled from the surface. So the effects on the k_La depend on the sorts of salts present in the medium.

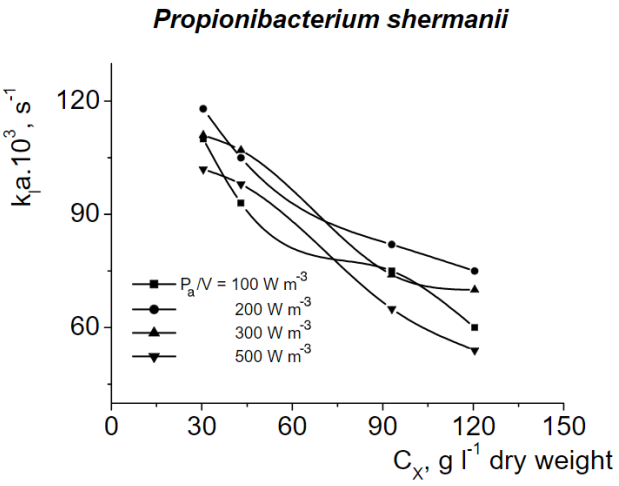

Fig. 4: The influence of biomass concentration on the k_La at different energy dissipation rates (Galaction et al., 2004)

Biomass

When biomass is produced or added to the medium, the viscosity rises, this has a negative effect on the k_La (Figure 2). Besides an increase in viscosity, adding biomass also creates a blocking effect for mass transfer by adsorption to the air bubble surface and lowering oxygen solubility (Galaction et al., 2004). Galaction et al. (2004) show a significant relationship between the biomass concentration and the k_La (Figure 4. Mota et al. (2011) reported a destabilisation of the homogeneous regime caused by solid particles in a bubble column. Because fermentation broths are complex media, it isn't easy to predict the exact effect they will have on the oxygen mass transfer inside the bubble column.

Proteins

Proteins adhere very strongly to the liquid surface and thus create a semi rigid interface (Xiao & Konermann, 2015). This leads to less new liquid that comes into contact with the gas at the bubble-liquid surface. This decreases the k_L. However, this effect is strongest for bubbles with a diameter of less than 3 mm. Furthermore, proteins prevent bubble coalescence by stabilizing the liquid layer between two bubbles. The latter effect is stronger in most cases so proteins are likely to have a positive effect on the mass transfer coefficient (Prins & Van't Riet, 1987).

Project scope

Although a lot of research has been done on the influence of the separate components on the mass transfer coefficient, very little research has been done on the effect of fermentation broth on the volumetric mass transfer coefficient. And, to the authors knowledge, no research has been done on the combination of fermentation broth with ethanol. This research aims to determine the effect of medium properties and the combination of ethanol with different types of media on the k_La in bubble columns. This will lead to a better understanding on how to increase this important parameter for more efficient syngas conversion. To achieve this, the influence of different medium properties on the bubble size, surface area, k_L and the k_La will be determined.

TABLE II: The different media that will be studied in this research.

Medium	Case	Study case
1	Water	+ Ethanol
2	Mineral medium	+ Ethanol
3	Fermentation broth from TUEwith *C. autoethanogenum*	+ Ethanol
4	Fermentation broth from WURwith *C. autoethanogenum*	+ Ethanol
5	Fermentation broth from TUDwith *C. autoethanogenum*	+ Ethanol
6	Fermentation broth from WURwith *R. rubrum*	+ Ethanol

II. Experimental methods

In this research, the influence of five different media, in combination with ethanol, on the k_La, the a and the k_L will be tested. The six different media are displayed in Table II. The fermentation broths are supplied by Delft University of Technology (TUD), Eindhoven University of Technology (TUE) and Wageningen University & Research (WUR). The experiments will be conducted in a bubble column with a diameter of 7.32 cm and a liquid height of 70 cm. Once the superficial velocity is determined, all experiments will be conducted in a homogeneous flow regime. The gasses that are used to sparge the column are air and nitrogen. All results will be statistically tested with a Welch's t-test or Pearsons correlation coefficient (Appendix VII).

Determination of the superficial gas velocity

The superficial gas velocity at which the experiment is conducted, has a big impact on the results. One of the most important effects is that it determines the flow regime of the bubble column. To make sure that the experiment is conducted in the homogeneous flow regime, the gas holdup was measured in water for different superficial velocities. Figure 5 shows the typical curve for the gas holdup for air-water systems in a bubble column. By plotting a graph of the gas holdup versus different superficial gas velocities, the regime transition point can be determined (Krishna et al. (1999); Kim et al. (2017)).

k_La determination

To determine the k_La, the dynamic gassing out method was used (Straathof & Heijnen, 2020). This method started with a column which was supplied with fresh air by a sparger at the bottom of the fermentor. The oxygen concentration in the liquid was measured every two seconds with an AppliSens DO probe. When the liquid was fully saturated with oxygen, the oxygen concentration of the liquid phase was at an equilibrium with the gas phase. This concentration was determined as c^*_{O2} and can be calculated with Henry's law (W. Henry, 1803):

$$c^*_{O_2.L} = H * p^{O_2} \tag{1}$$

$$p^{O_2} = y_{O_2} * P_g \tag{2}$$

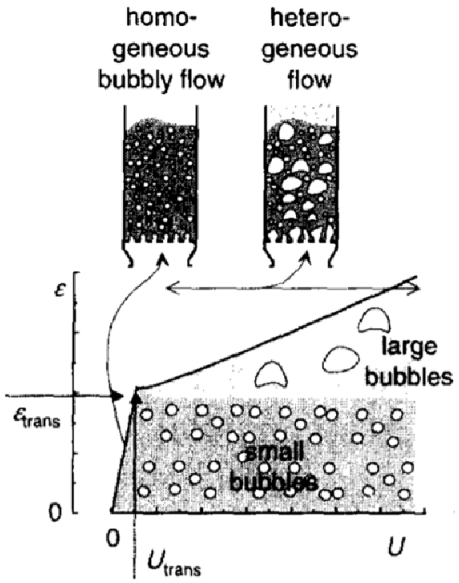

Fig. 5: Flow regimes and gas holdup for different superficial velocities in bubble columns (Krishna et al., 1999)

Following this, the inflow was switched to nitrogen gas, which strips the liquid of oxygen so that $c_{O_2.L} = 0$. Once this value was reached, the air flow is switched to air again, this causes $c_{O_2.L}$ to increase. The change in $c_{O_2.L}$ is calculated with a mass balance for oxygen:

$$\frac{d(V_L c_{O_2}(t))}{dt} = q_{O_2} N_x + k_L a (c^*_{O_2} - c_{O_2}(t)) V_L \quad (3)$$

In this experiment, q_{O2} was zero, as the used micro-organism is anaerobic. Because this is a batch process, V_L was constant and can be left out of the equation. This gives:

$$\frac{d(c_{O_2}(t))}{dt} = k_L a (c^*_{O_2} - c_{O_2}(t)) \quad (4)$$

Separation of variables gives:

$$\frac{d(c_{O_2}(t))}{c^*_{O_2} - c_{O_2}(t)} = \frac{-d(c^*_{O_2} - c_{O_2}(t))}{c^*_{O_2} - c_{O_2}(t)} = K_L a \; dt \quad (5)$$

Since $(dx)/x = d(lnx)$, this can be rewritten as:

$$d(ln(c^*_{O_2} - c_{O_2}(t))) = -K_L a \; dt \quad (6)$$

Integration between $t = 0$ and $t = t$, with the assumption that $k_L a$ is constant, gives:

$$ln(c^*_{O2} - c_{O2}(t)) - ln(c^*_{O2} - c_{O2}(0)) = -k_L a \; (t - 0) \quad (7)$$

This equation can be rewritten as:

$$ln\left[\frac{c^*_{O2} - c_{O2}(t))}{c^*_{O2} - c_{O2}(0)}\right] = -k_L a \; t \quad (8)$$

By plotting the left part of the equation against the time, the $k_L a$ is determined by taking the slope of the graph. The mean $k_L a$ values were calculated as the weighted mean of the measured values. The weights were assigned relative to the R^2 values. Appendix VII elaborates further on this.

In the case of the broth with *C. autoethanogenum* from TUD, q_{O_2} was not zero. The calculations for these $k_L a$ values can be found in Appendix IV.

Because the DO probes had a tendency to drift during the experiment, new calibrations were needed. Because it is not possible to compare measurements from different calibrations directly to each other, all measured values will be related to the $k_L a$ value of water for that day. Subsequently these values will be related to the first $k_L a$ value of water, which is assumed to be reliable.

Mixing time determination

There are multiple methods to measure the $k_L a$, each with their own advantages and disadvantages. The biggest downside of the dynamic gassing out method is that it assumes an ideal mixed gas and liquid phase. To ascertain this assumption, the mixing time should be lower than $1/k_L a$ (Merchuk et al., 1990). The mixing time was estimated by the following equation (Groen, 1994):

$$t_m = \frac{N_{mix} \, d_c^{2/3}}{\epsilon_{dissipation}^{1/3}} \quad (9)$$

$\epsilon_{dissipation}$ is the energy dissipation in the column, this is calculated by using the formula from Heijnen and Van't Riet (1984) and dividing it by the density of the medium:

$$\epsilon_{dissipation} = u_{G,s} \, g \quad (10)$$

N_{mix} is the mixing number, which is the product of the mixing time and the stirrer rotational speed. Because there is no stirrer present in a bubble column, the mixing number is estimated by the universal equation for the mixing number (Brennan & DJ, 1976):

$$N_{mix} = \alpha \, \beta^{-4/3} \, \gamma^{-1/3} \left(\frac{L_s}{h_L}\right)^2 \left(\frac{h_L}{d_c}\right)^2 \quad (11)$$

Groen (1994) simplifies this equation by taking 0.374 for α, 1 for $\frac{L_s}{h_L}$ and 0.28 for β (in a homogeneous flow regime). γ is a dimensionless viscosity parameter, which Groen calculates to be 39.1 for water and most fermentation broths. Because the mixing number was only used to evaluate the method of $K_L a$ measurement, the value of 39.1 was

taken for all media. This led to a dependency of the mixing number on the ratio between the liquid height and the column diameter. The mixing number, mixing time and $1/k_La$ for each medium were determined to evaluate if the assumption of an ideally mixed liquid state can be justified.

Determination of the interfacial area

To study the effects of the medium parameters on the k_L and the a separately, the interfacial area between the liquid and the gas phase was determined in each experiment. In order to determine the interfacial area, the Sauter mean bubble diameter was determined (Sauter, 1926). This was done by analysing pictures of the bubbles. The bubbles were photographed and analysed in two ways due to limited ranges of the measurement methods. Media without ethanol were photographed using a Canon EOS200D camera and media with ethanol were photographed using the SOPAT probe. The WUR *C. autoethanogenum* broth without ethanol was analysed with both methods to compare the results.

Using the SOPAT probe: For bubbles with a small diameter, the SOPAT Probe was used to take pictures of the bubbles. The pictures were analysed in Python using the circle Hough transformation method, where the assumption was made that all bubbles are perfect spheres. The script that was used for this can be found in Appendix V. This script gives the mean diameter of the bubbles and a plot of the bubble size distribution as output.

Using the Canon EOS200D: The pictures from the Canon were taken from outside the fermentor. Inside the column is a ruler that was used as a scale to convert pixels to mm. This way, the refraction of the light should not influence the measurements.

For bubbles that had a spherical shape, the diameter (d_b) was measured. The others were assumed to be spheroids. This means that they are symmetrical around the vertical/short axis. The long axis (d_a) and the short (d_c) axis were measured in pixels, using ImageJ. These axis, once converted to mm, are used to determine the volume and surface area of the bubble with (Wang & Fan, 2013):

$$V = \frac{\pi}{6\, d_a^2\, d_c} \tag{12}$$

$$A = 2\,\pi\, r_a^2 + \pi\, \frac{r_c^2}{e}\, ln\left(\frac{1+e}{1-e}\right) \tag{13}$$

Where e, the eccentricity of the bubble, is calculated by:

$$e = \sqrt{\frac{1 - r_c}{r_a^2}} \tag{14}$$

With this information, the Sauter bubble diameter can be calculated. This is the equivalent diameter of a sphere that has the same volume/surface ratio as the spheroid. This helps to compare the bubbles to each other and to determine the mean bubble size. It is calculated with:

$$d_{32} = 6\frac{V}{A} \tag{15}$$

TUE *C. autoethanogenum*	$c_x = 0.501\,OD - 0.074$	Hop (2021)
TUD *C. autoethanogenum*	$c_x = 0.392 * OD$	Schotsman (2021)

TABLE III: Equations to calculate the biomass dry weight (g_x/L) from OD values.

Using either d_b or d_{32}, the Sauter mean bubble diameter can be determined with:

$$d_{sv} = \sum p_i d_{b,i} \tag{16}$$

With this mean diameter, the interfacial area can be calculated:

$$A = \frac{6\epsilon}{d_{sv}} \tag{17}$$

ϵ is the gas holdup, this is the volume fraction of the gas in the total volume. It can be calculated by:

$$\epsilon = \frac{V_{tot} - V_L}{V_{tot}} \tag{18}$$

To determine the k_L, the total surface area should first be converted to the specific surface area (a):

$$a = A/V \tag{19}$$

Then, the k_L can be calculated by:

$$k_L = k_La/a \tag{20}$$

Medium characterisation

To link the k_La to the properties of the medium, these were also measured. The density was measured using the DMA^{TM} 5000 from Anton Paar. The viscosity was measured using the HAAKE Viscotester^{TM} 500 at 37 °C, with the NV sensor system.

The dynamic surface tension of the medium was determined with the BPT Mobile from KRÜSS. This gives the surface tension for bubbles with a surface age between 1 and 10000 ms. For this research, the mean value for the surface tension in the column is of interest, this was determined with the calculations in Appendix VI.

The cell density of the fermentation broth was determined in two ways: The first was by measuring the optical density at a wavelenght of 600 nm and with a path lengt of 10 mm. This was done using the DR3900 laboratory spectrophotometer from HACH. This value was converted to the cellular dry weight in g_x/mL with equations that have been determined in earlier experiments with the broths. This equation has been determined for TUD and TUE *C. autoethanogenum*. However, it is assumed that an estimation of the dry weight of WUR *C. autoethanogenum* can be made based on the equation from the broth from TUD. These equations are shown in Table III

The second way was to determine the dry weight of a known amount of fermentation broth. This was done following the protocol in Appendix VIII.

The protein concentration will be determined with the Pierce^{TM} BCA Protein Assay Kit, from ThermoFischer.

This assay consists of three steps. First Cu^{2+} ions from the copper(II) sulfate in the bicinchoninic acid (BCA) solution are reduced to Cu^{1+}. After this, each Cu^{1+} chelates with two molecules of BCA. This forms a purple complex which absorbs light at a wavelength of 562 nm. Because there is a linear relation between the absorption and the protein concentration, the protein concentration of the sample could be determined by comparing the absorbance with that of standards with a known protein concentration (Olson & Markwell, 2007). The standard manual for a 96 microwell plate, that is included with the kit, was followed for this assay (*Pierce*^{TM} *BCA Protein Assay Kit*, 2020).

Lastly, samples from the investigated fermentation broth were checked under the microscope to verify the viability of the cells (live or dead). This showed if the cells were still alive. Dead cells have an influence on the viscosity and the surface tension because they disintegrate and thus alter the composition of the broth. For results that are applicable to bubble columns with an active fermentation process, the cells should still be alive.

III. Results

Superficial gas velocity determination

To determine the superficial gas velocity at which this experiment was conducted, the gas holdup was determined for different superficial velocities. By analysing the slope of the graph in Figure 6, it was determined that the homogeneous regime takes place until a superficial gas velocity of 0.54 cm/s. Before this point, the slope of the graph is higher than after this point, this indicates that the homogeneous regime ends there. (Heijnen & Van't Riet, 1984) proposed the following two equations for the relation between the gas holdup and the superficial velocity in air water-systems. One for a homogeneous flowregime and one for a heterogeneous flowregime.

$$\epsilon_{homogeneousregime} = \frac{u_{G,s}}{0.25} \tag{21}$$

$$\epsilon_{heterogeneousregime} = 0.6\, u_{G,s}^{0.7} \tag{22}$$

Both these equations also plotted in Figure 6. The experimental values follow the homogeneous equation until a superficial velocity of around 0.59 cm/s. The slope of the graph changes at 0.54 cm/s, indicating that the column is operating in a homogeneous flow regime until that point. Addition of biomass might have an destabilizing effect on the homogeneous regime. To ensure a homogeneous regime in all media, the superficial gas velocity was set at 0.191 cm/s.

Medium characterisation

Four different fermentation broths were used in this research. Table IV shows the most important aspects to characterise these broths. Appendix I shows all the measured properties for each medium. The ethanol concentration in the broths from TUE and WUR with *C. autoethanogenum* are zero or very small and thus assumed to be negligible

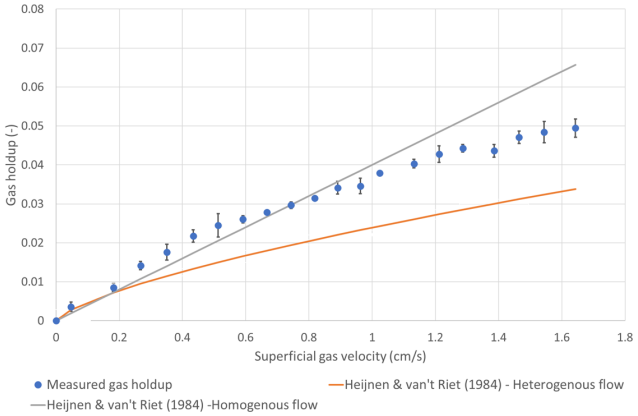

Fig. 6: *The gas holdup for different superficial velocities. Plotted with equations for a homogeneous and heterogeneous flow regime, as proposed by Heijnen and Van't Riet (1984).*

(Appendix I). The ethanol concentration in the TUD *C. autoethanogenum* broth is unknown but it is assumed that this value is also negligible.

Mass transfer parameters

The specific surface area, k_L and k_La were determined for all media. Because the powerful reducing agent in the medium of WUR *C. autoethanogenum* probably interfered with the probes, these values for the k_La and k_L can't be trusted and are thus discarded (see Appendix IV for a further explanation). The k_La of the TUD *C. autoethanogenum* broth was determined with the method as described in Appendix IV because there was oxygen consumption in this medium. In all cases, the addition of ethanol increased the specific surface area and the k_La value (Figure 7a & c). The increase in interfacial area was the most prominent in the broth with *R. rubrum* from WUR. This broth differs from the other broths in the fact that it has the lowest protein concentration and the highest biomass concentration, which might have an influence. After the addition of ethanol, the k_La increased the most in water. In all cases, ethanol had a decreasing effect on the k_L, this is probably due to the earlier described blocking effect on mass transfer at the gas-liquid interface (Figure 7b).

Without ethanol, mineral medium had a higher k_La and specific surface area than water. With ethanol, these values were higher for water. In both cases, the k_L was lower in the cases with mineral medium (7). This shows that in the case without ethanol, the increase in surface area compared to that of water has a bigger impact. While, in the case with ethanol, the decrease in k_La had the biggest impact.

Compared to water, a decrease in the k_La was observed in the experiments with TUE *C. autoethanogenum* and WUR *R. rubrum* with and without ethanol. The TUD *C. autoethanogenum* broth led to a increase in k_La in the test case without ethanol and to a decrease in the test case with ethanol (Figure 7c). In all cases, expect the TUD *C. autoethanogenum* broth with ethanol, the presence of biomass led to an increase in the surface area (Figure 7a).

TABLE IV: Properties of the fermentation broths

Medium	Cultivation method	Cell viability[b]	Initial substrate composition	Biomass concentration (g_x/L)	Protein concentration $(\mu g/mL)$
TUE *C. autoethanogenum*	Spinning disk reactor, effluent	Dead	100% CO	0.2457	1278.1
WUR *R. rubrum*	CSTR effluent[a]	Alive	50% CO, 40%H_2, 10% CO_2	0.0874[c]	62.4
WUR *C. autoethanogenum*	Batch botles cultivation	Alive	50% CO, 40%H_2, 10% CO_2	0.5043[c]	563.4
TUD *C. autoethanogenum*	CSTR effluent[a]	Alive	50% CO, 50% H_2	0.0613	369.1

[a] collected over 9 days (WUR *R. rubrum*) and 4 days (TUD *C. autoethanogenum* under anaerobic conditions. [b] Confirmed by microscope observation (Appendix III). [c] Estimated from OD, using the correlation in Table III.

The results of the TUD *C. autoethanogenum* broth are very close to those of the mineral medium. This could be because of the low biomass and protein concentration (Table IV).

In all cases, the k_L decreased when minerals or biomass are present. This is due to the blocking effect of the surfactants on the mass transfer at the gas-liquid interface. Figure 8 shows the relationship between the biomass concentration and the k_L (p=0.0023). In the experiments with the WUR and TUE *C. autoethanogenum* broths, the decrease in k_L has a bigger impact on the k_La than the increase in surface area, leading to a lower k_La than that of water. In the experiment with the TUD *C. autoethanogenum* broth, the increase in surface area had a bigger impact than the decrease in k_L, leading to a higher k_La than that of water.

Adding surface active compounds had a positive effect on the specific surface area (Figure 9a, p=0.010) and the gas holdup (Figure 9b, p=0.005) and a negative effect on the mean bubble size (Figure 9c, p=0.007). Lowering the surface tension leads to less bubble coalescence and thus smaller bubbles and a bigger surface area and gas holdup.

k_La in respect to the mixing time

To make sure that the assumption of an ideally mixed liquid phase is justified, the mixing time should be lower that $1/k_La$ in all study cases. The bubble column that is used in this research has a diameter of 7.32 cm and a liquid height of 69 cm. This leads to a mixing number of $N_{mix} = 53.45$. This gives a mixing time of 35.17 seconds, which is lower than $1/k_La = 154.9s$ of water. The value of $1/k_La$ of all the media can be found in Table V. The mixing time is lower than $1/k_La$ for all media except for water with ethanol. This means that the assumption of a perfectly mixed liquid phase can be made for all cases except ethanol.

Bubble size distribution

For all media, the mean bubble diameter and the bubble size distribution have been determined (Figure 10, Appendix II, Appendix I). In all cases, expect WUR *C. autoethanogenum*, the addition of ethanol leads to a decrease in bubble diameter (p<<0.05). The bubble size distribution plots in Appendix II and the standard deviations in Figure 10 show that the distribution of the bubble diameters is wider in the media without ethanol. So the addition of ethanol leads to more homogeneously distributed bubbles. The expectation that this leads to a bigger specific area is confirmed in the results of this research (Figure 7, Appendix I). Figure 9

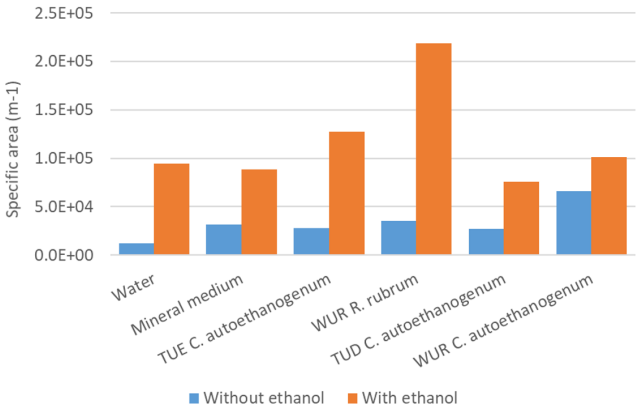

(a) Specific surface area

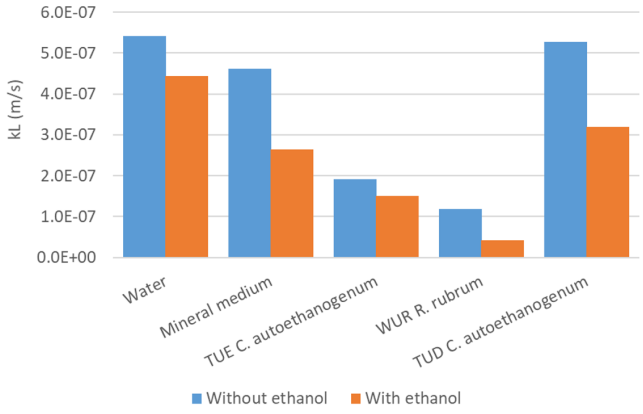

(b) k_L

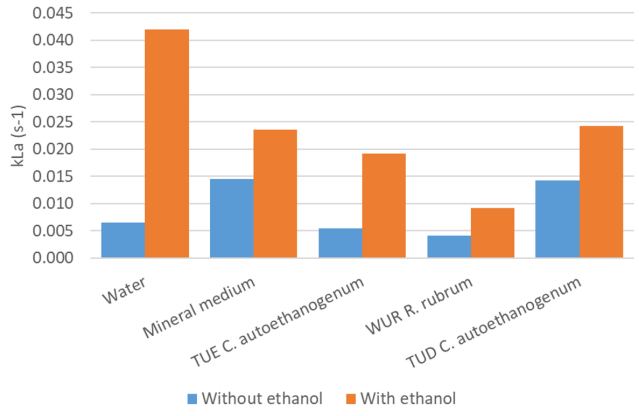

(c) k_La

Fig. 7: The specific surface area, k_L and k_La for all media.

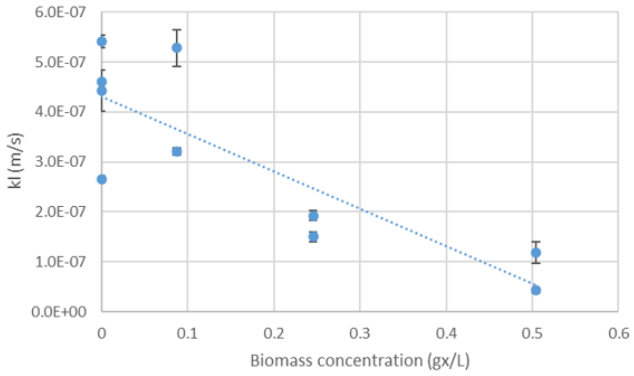

Fig. 8: The relation between the biomass concentration and the k_L.

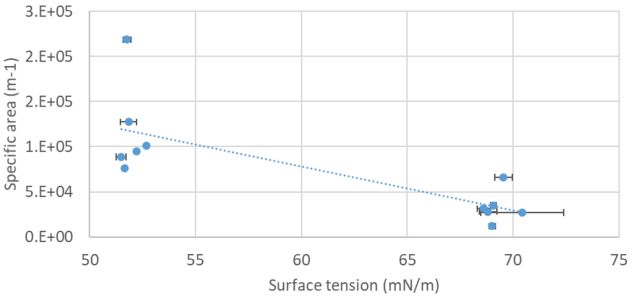

(a) Specific surface area

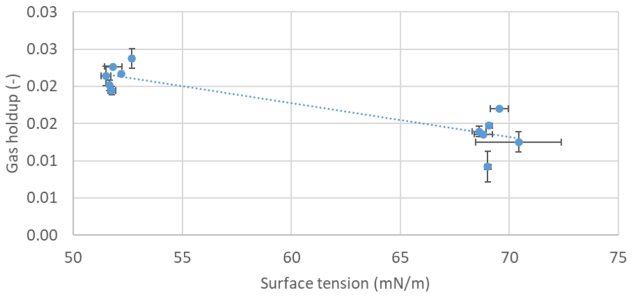

(b) Gas holdup

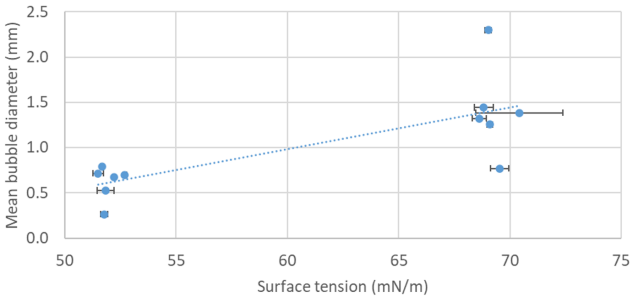

(c) Bubble diameter

Fig. 9: Effect of surface tension on the surface area, the total gas holdup and the bubble diameter in the column.

TABLE V: Value for $1/k_La$ for different media

Medium	**1/k$_L$a**
Water	154.9
Water, 5% ethanol	23.8
Mineral medium	68.8
Mineral medium, 5% ethanol	42.5
TUE *C. autoethanogenum*	184.9
TUE *C. autoethanogenum*, 5% ethanol	52.3
WUR *R. rubrum*	240.9
WUR *R. rubrum*, 5% ethanol	108.51
WUR *C. autoethanogenum*	111.4
WUR *C. autoethanogenum*	135.1
TUD C. autoethanogenum	70.0
TUD C. autoethanogenum, 5% ethanol	41.2

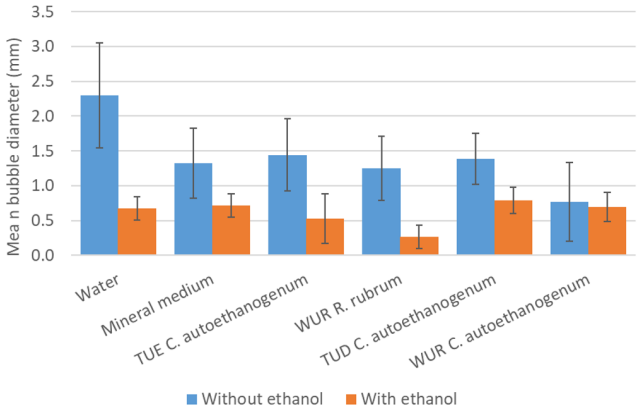

Fig. 10: The mean bubble size in different media

shows that this effect is probably a result of the lower surface tension in the media with ethanol.

Both methods for picturing the bubbles have their own working range, so it's hard to compare the results with each other. The fermentation broth with *C. autoethanogenum* had bubbles that were on the border between both ranges, these bubbles are evaluated using both methods. This way, it can be seen if the methods give the same results. With the method using the Canon camera, the mean diameter was 0.7692. With the method using the SOPAT probe, this was 0.7753. The bubble size distribution for both methods is shown in Figure 11

IV. Discussion

The aim of this study was to evaluate the effects of medium properties and the addition of ethanol on the specific surface area, k_L and k_La. It is shown that ethanol and the broth with *C. autoethanogenum* have an increasing effect on the k_La and all other fermentation broths have a decreasing effect on the k_La. The most important results will be discussed below.

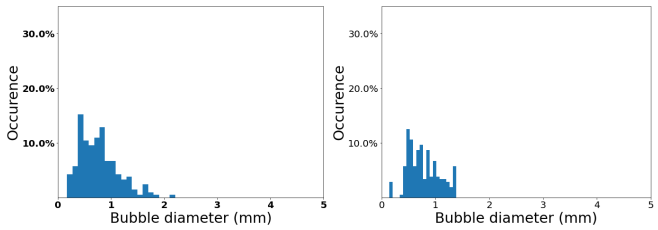

(a) Canon method (b) SOPAT method

Fig. 11: Bubble size distributions of *C. autoethanogenum*, pictured with a Canon camera and a SOPAT probe

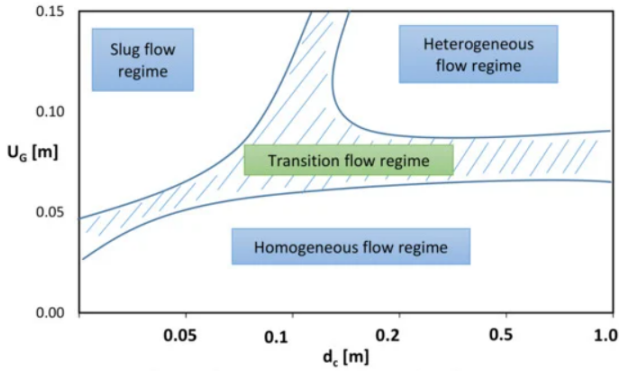

Fig. 12: Flow regimes at different column diameters and superficial velocities (Shah et al., 1982).

Superficial velocity determination

By measuring the gas gas holdup at different superficial gas velocities, the gas flow rate at which a homogeneous regime takes place was determined. A change in the slope can be seen from a superficial velocity from 0.54 cm/s. This finding corresponds to equations (23) and (24) by Heijnen and Van't Riet (1984). Shah et al. (1982) mapped the correlation between the column diameter, gas flow and the flow regime. As can be seen in Figure 12, at a diameter of 0.07 m, a homogeneous flow takes place until 6 cm/s. Based on these sources, a superficial gas velocity of 0.191 cm/s should be well in the range of a homogeneous flow regime. However, it should be noted that there is no real homogeneous regime in the column. Because the sparger inlet is on one side of the column, this side has a higher bubble density. This will most likely lead to a uneven radial distribution of the k_La in the column. For future research the sparger should be in the middle of the column to ensure a real homogeneous regime.

Medium characterisation

All the media were characterised by determining several parameters and evaluating the viability of the cells. The media were all very close in their value for surface tension and viscosity (Appendix I). To give clearer and more widely applicable results on the effect of these parameters, a wider range should be tested. Due to time constraints and the laborious methods used, it was not possible to determine the viscosity, density, dry weight and density on the same day as the k_La measurements. Some of these values might have changed due to the deterioration of dying cells. The deterioration of cells might have particularly impacted the viscosity of the broths. To accurately determine the conditions inside the column, these parameters should all be measured right away.

Mass transfer parameters

For all media, the addition of ethanol increased the k_La and the surface area and decreased the k_L (Figure 7). This is in line with earlier research from Öztürk et al. (1987), Wagenaar (2021) and Jamialahmadi and Müller-Steinhagen (1992). This effect was the most pronounced in water, this is probably because at a certain surfactant concentration, the critical micelle concentration (CMC) is reached. At this concentration, the entire surface is satisfied with surfactants, meaning that added surfactants will localise in the bulk or in a second surface layer where they have less influence (Mancy & Okun, 1960). In the media that already had surfactants, this CMC is reached faster, leading to a smaller difference in k_La than in water.

A higher biomass concentration is correlated with decreasing k_L values. These effects are not due to viscosity, as no correlation between the viscosity and the k_L was found in this research (Appendix I). It is most likely that these effects are due to the blocking effect of cells that adhere to the bubble surface (Allen & Robinson, 1989). The decrease k_L with the addition of surface active compounds correlates with the hypothesis of Godbole et al. (1983). This means that the blocking effect of surface active compounds stronger is than the "shuttle effect", as described by Pegram and Record (2007).

An interesting observation is that the TUD fermentation broth with *C. autoethanogenum* was the only fermentation broth that had a higher k_La than water in the test case without ethanol. This is probably due to the low biomass concentration (0.087 g_x/L), IV). At this concentration, the negative influence of biomass concentration on the k_L is compensated by the positive effect of the minerals and other surfactants on the surface area.

The experimental k_La values are compared to k_La values that are calculated with empirical correlations from several papers in Figure 13 (The equations can be found in Appendix VII). The blue line in this figure is the axis where the values of the equations would lie if they gave the same result as the values in this research. These empirical correlations are not able to predict the k_La value that was found in these experiments. This is not very surprising since these equations mostly rely on parameters that are more or less in the same range for all media. It is clear that the k_La is not only dependent on these parameters but that more factors play a role. Since fermentation broths are complex media, it is advised to evaluate the influence of all components and parameters to accurately predict the k_La.

An important assumption that is made is that the first values for the k_La in water can be used as reliable values

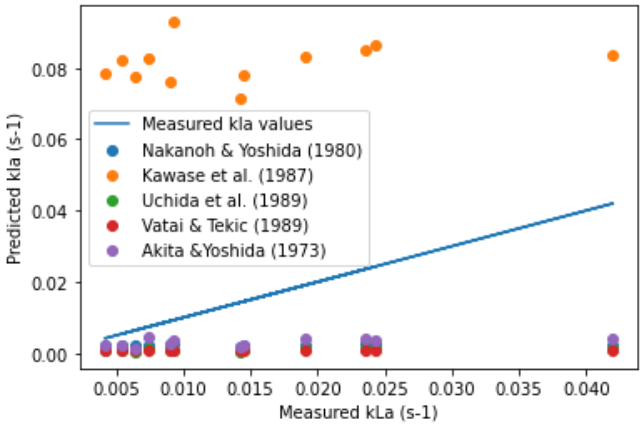

Fig. 13: Comparison of the measured k_La values and values from empirical correlations from various papers.

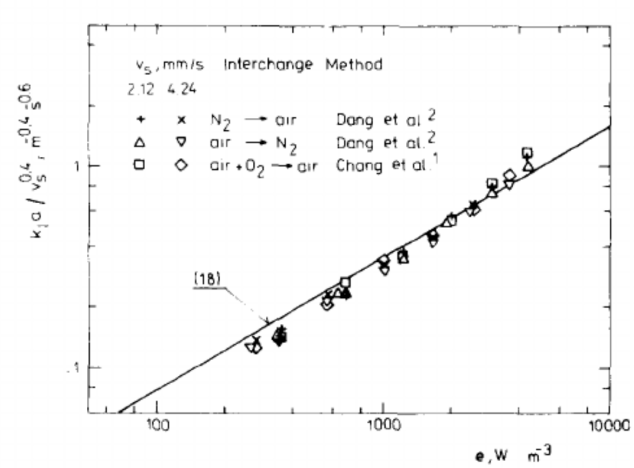

(a) Coalescing liquids

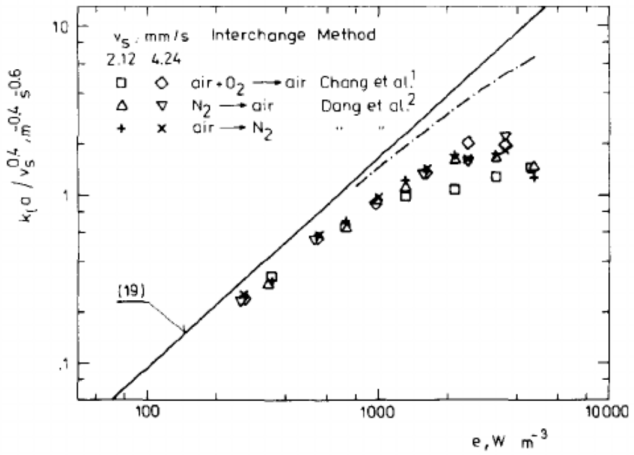

(b) Non-coalescing liquids

Fig. 14: Comparison between the dynamic gassing out method and a reference equation of a correct k_La measurement method for coalescing and non-coalescing liquids. At different energy dissipation values.

to refer the rest of the values to. Even though several measurements of this value were conducted, this value needs to be established further to be able to see this as the real value of the k_La.

Method of k_La measurement

For all media, the assumption that the medium was ideally mixed was justified, because in all cases $1/k_La >> t_m$ (Table V). Linek et al. (1991) show that the dynamic gassing out method gives a wrong value for the k_La at high values of power dissipation. These results are more pronounced in coalescing liquids than in non-coalescing liquids (Figure 14). The dissipation rate of the column in this experiment can be calculated with:

$$e = \rho_L \, g \, u_{G,s} \; W/m^3 \tag{23}$$

With liquid densities between 984.36 and 997.97 kg/m^3 (Appendix I), this value ranges between 18.51 and 18.76 W/m^3. In this range, the variation in k_La between the dynamic gassing out method and the real k_La value is very small. Thus it is assumed that the k_La value of this experiment is close enough to the real value for the results to be significant (Figure 14).

The mixing time is lower than $1/k_La$ for most cases, except for water with ethanol (Table V). This means that for that case, it can't be assumed that the measured k_La value is the same as that of the column as a whole. For that case, a method that does not assume an ideally mixed liquid phase should be used.

Another important factor in determining if the right method is used is the probe response time. This should be smaller than $0.05/k_La$ (Straathof & Heijnen, 2020). Table VI shows this value for each medium. For most media, this value is lower than the probe response time, which is 2 seconds. However, the k_La for water with 5% Ethanol is too high and thus does not give enough data points to accurately determine the k_La. In future studies, a probe with maximum response time of one second should be used to make sure that enough data points can be obtained.

TABLE VI: Value for $0.05/k_La$ for different media

Medium	**1/kla (s)**
Water	7.75
Water, 5% ethanol	1.19
Mineral medium	3.44
Mineral medium, 5% ethanol	2.13
TUE C. autoethanogenum	9.25
TUE C. autoethanogenum, 5% ethanol	2.62
WUR R. rubrum	12.04
WUR R. rubrum, 5% ethanol	5.43
WUR C. autoethanogenum	5.57
WUR C. autoethanogenum, 5% ethanol	6.75
TUD C. autoethanogenum	3.50
TUD C. autoethanogenum, 5% ethanol	2.06

Based on the aforementioned determinations, the dynamic gassing out method is rightfully used to determine the k_La. However, this method is still highly dependent on the oxygen probe used . The k_La values for some of the media in this experiment diverged a lot from their duplicates or triplicates. For future research multiple, reliable probes should be used for this method of k_La measurement.

Besides the dependency of the probe, this method assumes a homogeneous distribution of the k_La. Multiple articles have proven the opposite to be the case (Kulkarni (2007) León-Becerril and Maya-Yescas (2010) Deckwer et al. (1974) Gourich et al. (2008)). The k_La is highly dependent on the position in the column, so for a complete understanding of the k_La, this should be measured at multiple positions.

Another drawback of the dynamic gassing out method is that it comes with extra complications when oxygen consumption takes place in the column. In that case, the qO_2N_x term in equation (3) won't be zero. To determine the k_La in these cases, the oxygen consumption rate should be determined. Appendix IV elaborates more on this subject. During this experiment it was noticed that the media with cysteine, a reducing agent, influenced the probe. After using the probe in these media, it needed about a day of sparging with air in water to return back to the original state. For media with cysteine of other powerful reducing agents, it is advised to use another method of k_La measurement. For example off-gas analysis or measuring the CO_2 concentration. Appendix III elaborates further on this.

Bubble size distribution

In all cases, the mean bubble size decreased when ethanol was added to the media (Figure 15). This is in accordance with the results of Besagni et al. (2016) and Jamialahmadi and Müller-Steinhagen (1992). The bubble size also decreased when biomass or mineral medium is added, since these medias contain surface active compounds this also affects the bubble size. Thus, the results in Figure 15 and 9 compare to each other.

Because of the limited range of the bubble measurement methods, two methods were used in this research. Both with their own advantages and disadvantages. For example, the analysis of the pictures from the SOPAT probe is very reliable as it is done by computational methods (see Appendix V). However, this method only measures bubbles at one point in the column, while the pictures that were taken with the Canon camera enable analysis of bubbles over a bigger part of the column. Especially for coalescing liquids, water in this case, this is a problem. McClure et al. (2013) shows that the bubble size in water varies a lot depending on where in the column the bubbles are measured. Because of bubble coalescence, the bubble size increases with height at which it is measured. Yan et al. (2020) also showed that the bubble size depends on the radial position in the column. Besides this, the SOPAT probe can only measure bubbles up to 1.4 mm. So if bigger bubbles than this were present in the column, they are not included in the determination of the mean bubble size. For example, the bubble size distribution plot of TUE *C. autoethanogenum* with 5% ethanol (Figure 15f), does suspect that there are bubbles bigger than 1.4 mm present in the liquid.

Both methods were compared to each other in the broth with WUR *C. autoethanogenum*. Figure 11 shows the difference in the bubble size distributions determined by the method using the SOPAT probe and the Canon camera. The mean diameters were close in value but not the same (Δd=0.0061 mm). Even though the SOPAT method can only measure bubbles up to 1.4 mm and the Canon method has no maximum bubble size, the mean bubble diameter, measured with the SOPAT method, is higher that that measured with the Canon method. This does suspect that in the Canon method, smaller bubbles might be overlooked since they don't appear as clear on the pictures as the bigger bubbles. There is also a difference in the bubble size distributions. However, the difference between the two method is small enough to compare both methods with each other. For future research it is advised to use computational analysing methods on pictures of the Canon camera. This ensures an equal analysis of all bubbles and no exclusions based on bubble size.

V. Conclusion

This research shows that the addition of ethanol to various media has an increasing effect on the specific area and the k_La and a decreasing effect on the k_L. A negative correlation between the biomass concentration and the k_L has been found. It is expected that this is mainly due to the blocking effect of biomass at the gas-liquid interface. The decrease in surface tension due to the presence of surface active compounds led to an increase in the specific area and gas holdup and to a decrease in mean bubble diameter in the bubble column. These results showed that it is not possible to determine the k_La with the measured properties of the media. Fermentation broths are complex media with various components that affect the k_La. This research gives insight in the factors that influence the k_La, which contributes to the optimisation of syngas fermentation processes. However, more research on fermentation broth properties on the k_La should be done to gain a more complete insight in the mechanism of gas-liquid mass transfer in bioprocesses.

NOMENCLATURE

Symbol	Definition	Units
A	Interfacial area	m^2
a	Specific interfacial area	$m^2\, m^{-3}$
A	Surface area	m^2
c	Concentration	$mg\, L^{-1}$
d	Diameter	m
g	Gravitational acceleration	$m\, s^{-2}$
h	height	m
H	Henry's constant	$mol\, m^3\, bar$
k_L	Liquid phase oxygen mass transfer coefficient	$m\, sec^{-1}$
$k_L a$	Volumetric mass transfer coefficient	s^{-1}
L_s	Length of streamline	m
N_{mix}	Mixing number	$[-]$
N_x	Amount of biomass	mol
P	Total pressure of phase	bar
p^i	Partial pressure of component *i*	bar
p_i	Fraction of bubbles with diameter *di*	$[-]$
q_i	Biomass specific conversion rate of component *i*	$mol\, mol_x^{-1}\, s^{-1}$
r	Radius	m
t	Time	s
T	Temperature	$^\circ K$
$u_{G,s}$	Gas superficial velocity	$m\, s^{-1}$
V	Volume	m^3
y_i	Molar fraction of component *i* in gas phase	$[-]$
ϵ	Gas holdup	$[-]$
ϵ	Energy dissipation	$W\, kg^{-1}$ or; $W\, m^{-3}$
γ	Shear rate	s^{-1}
ρ	Density	$g\, L^{-1}$
σ	Surface tension	$N\, m^{-1}$
η_L	Kinematic viscosity of liquid phase	$m^2\, s^{-1}$
	Subscripts and Superscripts	
b	Bubble	
circle	Circle	
column	Column	
d	Droplet	
G	Gas	
i	Component i	
L	Liquid	
m	mixing	
O2	Oxygen	
sv	Sauter mean bubble diameter	
Tot	Total	
32	Sauter bubble diameter	
*	At equilibruim phase	

References

Abubackar, H. N., Veiga, M. C., & Kennes, C. (2011). Biological conversion of carbon monoxide: Rich syngas or waste gases to bioethanol. *Biofuels, Bioproducts and Biorefining*, *5*(1), 93–114.

Akita, K., & Yoshida, F. (1973). Gas holdup and volumetric mass transfer coefficient in bubble columns. effects of liquid properties. *Industrial & Engineering Chemistry Process Design and Development*, *12*(1), 76–80.

Allen, D. G., & Robinson, C. W. (1989). Hydrodynamics and mass transfer in aspergillus niger fermentations in bubble column and loop bioreactors. *Biotechnology and bioengineering*, *34*(6), 731–740.

Alper, E., & Öztürk, S. (1986). The effect of activated carbon loading on oxygen absorption into aqueous sodium sulphide solutions in a slurry reactor. *The Chemical Engineering Journal*, *32*(2), 127–130.

Alper, E., Wichtendahl, B., & Deckwer, W.-D. (1980). Gas absorption mechanism in catalytic slurry reactors. *Chemical Engineering Science*, *35*(1-2), 217–222.

Besagni, G., Inzoli, F., De Guido, G., & Pellegrini, L. A. (2016). Experimental investigation on the influence of ethanol on bubble column hydrodynamics. *Chemical Engineering Research and Design*, *112*, 1–15.

Brennan, D., & DJ, B. (1976). Impeller mixing in vessels. experimental studies on the influence of some parameters and formulation of a general mixing time equation.

Deckwer, W.-D., Burckhart, R., & Zoll, G. (1974). Mixing and mass transfer in tall bubble columns. *Chemical Engineering Science*, *29*(11), 2177–2188.

Dukhin, S. S., Kretzschmar, G., & Miller, R. (1995). *Dynamics of adsorption at liquid interfaces: Theory, experiment, application*. Elsevier.

Eastoe, J., & Dalton, J. (2000). Dynamic surface tension and adsorption mechanisms of surfactants at the air–water interface. *Advances in colloid and interface science*, *85*(2-3), 103–144.

Galaction, A.-I., Cascaval, D., Oniscu, C., & Turnea, M. (2004). Prediction of oxygen mass transfer coefficients in stirred bioreactors for bacteria, yeasts and fungus broths. *Biochemical Engineering Journal*, *20*(1), 85–94.

Garcia-Ochoa, F., & Gomez, E. (2009). Bioreactor scale-up and oxygen transfer rate in microbial processes: An overview. *Biotechnology advances*, *27*(2), 153–176.

Godbole, S., Schumpe, A., & Shah, Y. (1983). Hydrodynamics and mass transfer in bubble columns: Effect of solids. *Chemical Engineering Communications*, *24*(4-6), 235–258.

Gourich, B., Vial, C., El Azher, N., Soulami, M. B., & Ziyad, M. (2008). Influence of hydrodynamics and probe response on oxygen mass transfer measurements in a high aspect ratio bubble column reactor: Effect of the coalescence behaviour of the liquid phase. *Biochemical Engineering Journal*, *39*(1), 1–14.

Groen, D. J. (1994). Macromixing in bioreactors. *LIFE*, *27*.

Heijnen, J., & Van't Riet, K. (1984). Mass transfer, mixing and heat transfer phenomena in low viscosity bubble column reactors. *The Chemical Engineering Journal*, *28*(2), B21–B42.

Henry, & Craig, V. S. (2010). The link between ion specific bubble coalescence and hofmeister effects is the partitioning of ions within the interface. *Langmuir*, *26*(9), 6478–6483.

Henry, W. (1803). Iii. experiments on the quantity of gases absorbed by water, at different temperatures, and under different pressures. *Philosophical Transactions of the Royal Society of London*, (93), 29–274.

Huamán, A. (n.d.). Hough circle transform. https://docs.opencv.org/4.5.3/d4/d70/tutorial_hough_circle.html

Huang, J., & Saito, T. (2017). Influences of gas–liquid interface contamination on bubble motions, bubble wakes, and instantaneous mass transfer. *Chemical Engineering Science*, *157*, 182–199.

Jamialahmadi, M., & Müller-Steinhagen, H. (1992). Effect of alcohol, organic acid and potassium chloride concentration on bubble size, bubble rise velocity and gas hold-up in bubble columns. *The Chemical Engineering Journal*, *50*(1), 47–56.

Jia, X., Hu, W., Yuan, X., & Yu, K. (2014). Influence of the addition of ethanol to the gas phase on co2 absorption in a bubble column. *Industrial & Engineering Chemistry Research*, *53*(24), 10216–10224.

Kantarci, N., Borak, F., & Ulgen, K. O. (2005). Bubble column reactors. *Process biochemistry*, *40*(7), 2263–2283.

Kawase, Y., Halard, B., & Moo-Young, M. (1987). Theoretical prediction of volumetric mass transfer coefficients in bubble columns for newtonian and non-newtonian fluids. *chemical Engineering science*, *42*(7), 1609–1617.

Kim, J. Y., Kim, B., Nho, N.-S., Go, K.-S., Kim, W., Bae, J. W., Jeong, S. W., Epstein, N., & Lee, D. H. (2017). Gas holdup and hydrodynamic flow regime transition in bubble columns. *Journal of industrial and engineering chemistry*, *56*, 450–462.

Kluytmans, J., Van Wachem, B., Kuster, B., & Schouten, J. (2003). Mass transfer in sparged and stirred reactors: Influence of carbon particles and electrolyte. *Chemical Engineering Science*, *58*(20), 4719–4728.

Krishna, R., Ellenberger, J., & Maretto, C. (1999). Flow regime transition in bubble columns. *International communications in heat and mass transfer*, *26*(4), 467–475.

Kulkarni, A. A. (2007). Mass transfer in bubble column reactors: Effect of bubble size distribution. *Industrial & engineering chemistry research*, *46*(7), 2205–2211.

León-Becerril, E., & Maya-Yescas, R. (2010). Axial variation of mass transfer volumetric coefficients in bubble

column bioreactors. *Chemical Product and Process Modeling*, *5*(1).

Lessard, R. R., & Zieminski, S. A. (1971). Bubble coalescence and gas transfer in aqueous electrolytic solutions. *Industrial & Engineering Chemistry Fundamentals*, *10*(2), 260–269.

Linek, V., Sinkule, J., & Benes, P. (1991). Critical assessment of gassing-in methods for measuring kla in fermentors. *Biotechnology and bioengineering*, *38*(4), 323–330.

Mancy, K., & Okun, D. (1960). Effects of surface active agents on bubble aeration. *Journal (Water Pollution Control Federation)*, 351–364.

McClure, D. D., Kavanagh, J. M., Fletcher, D. F., & Barton, G. W. (2013). Development of a cfd model of bubble column bioreactors: Part one–a detailed experimental study. *Chemical Engineering & Technology*, *36*(12), 2065–2070.

Merchuk, J., Yona, S., Siegel, M., & Zvi, A. B. (1990). On the first-order approximation to the response of dissolved oxygen electrodes for dynamic kla estimation. *Biotechnology and bioengineering*, *35*(11), 1161–1163.

Mota, A., Vicente, A. A., & Teixeira, J. (2011). Effect of spent grains on flow regime transition in bubble column. *Chemical engineering science*, *66*(14), 3350–3357.

Naik, S. N., Goud, V. V., Rout, P. K., & Dalai, A. K. (2010). Production of first and second generation biofuels: A comprehensive review. *Renewable and sustainable energy reviews*, *14*(2), 578–597.

Nakanoh, M., & Yoshida, F. (1980). Gas absorption by newtonian and non-newtonian liquids in a bubble column. *Industrial & Engineering Chemistry Process Design and Development*, *19*(1), 190–195.

Olson, B. J., & Markwell, J. (2007). Assays for determination of protein concentration. *Current protocols in protein science*, *48*(1), 3–4.

Öztürk, S., Schumpe, A., & Deckwer, W.-D. (1987). Organic liquids in a bubble column: Holdups and mass transfer coefficients. *AIChE journal*, *33*(9), 1473–1480.

Park, S. H., Park, C., Lee, J., & Lee, B. (2017). A simple parameterization for the rising velocity of bubbles in a liquid pool. *Nuclear Engineering and Technology*, *49*(4), 692–699.

Pegram, L. M., & Record, M. T. (2007). Hofmeister salt effects on surface tension arise from partitioning of anions and cations between bulk water and the air-water interface. *The journal of physical chemistry B*, *111*(19), 5411–5417.

PierceTM bca protein assay kit. (2020). ThermoScientific. Illinois, USA.

Prins, A., & Van't Riet, K. (1987). Proteins and surface effects in fermentation: Foam, antifoam and mass transfer. *Trends in biotechnology*, *5*(11), 296–301.

Ruzicka, M., Drahos, J., Mena, P., & Teixeira, J. (2003). Effect of viscosity on homogeneous–heterogeneous flow regime transition in bubble columns. *Chemical Engineering Journal*, *96*(1-3), 15–22.

Sauter, J. (1926). Determining size of drops in fuel mixture of internal combustion engines.

Schotsman, F. (2021). *Cultivation of clostridium autoethanogenum for syngas fermentation optimization*.

Shah, Y., Kelkar, B. G., Godbole, S., & Deckwer, W.-D. (1982). Design parameters estimations for bubble column reactors. *AICHE journal*, *28*(3), 353–379.

Shaikh, A., & Al-Dahhan, M. H. (2007). A review on flow regime transition in bubble columns. *International Journal of Chemical Reactor Engineering*, *5*(1).

Springer, E. K. (2009). *O2 measurement guide*. Hamilton.

Straathof, A., & Heijnen, J. *Chemical biotechnology reader, mst-cbt*. 2020.

Sun, X., Atiyeh, H. K., Huhnke, R. L., & Tanner, R. S. (2019). Syngas fermentation process development for production of biofuels and chemicals: A review. *Bioresource Technology Reports*, *7*, 100279.

Suresh, S., Srivastava, V. C., & Mishra, I. (2009). Techniques for oxygen transfer measurement in bioreactors: A review. *Journal of Chemical Technology & Biotechnology: International Research in Process, Environmental & Clean Technology*, *84*(8), 1091–1103.

Taguchi, H. (1966). Dynamic measurement of the volumetric oxygen transfer coefficient in a fermentation system. *J. Ferment. Technol.*, *44*, 881–889.

Thobie, C., Gadoin, E., Blel, W., Pruvost, J., & Gentric, C. (2017). Global characterization of hydrodynamics and gas-liquid mass transfer in a thin-gap bubble column intended for microalgae cultivation. *Chemical Engineering and Processing: Process Intensification*, *122*, 76–89.

Uchida, S., Tsuyutani, S., & Seno, T. (1989). Flow regimes and mass transfer in counter-current bubble columns. *The Canadian Journal of Chemical Engineering*, *67*(5), 866–869.

Vatai, G., & Tekić, M. (1989). Gas hold-up and mass transfer in bubble columns with pseudoplastic liquids. *Chemical Engineering Science*, *44*(10), 2402–2407.

Wagenaar, E. (2021). *Influence of ethanol on the bubble size and the gas-liquid mass transfer of oxygen*.

Wang, D., & Fan, L.-S. (2013). Particle characterization and behavior relevant to fluidized bed combustion and gasification systems. *Fluidized bed technologies for near-zero emission combustion and gasification* (pp. 42–76). Elsevier.

Weissenborn, P. K., & Pugh, R. J. (1995). Surface tension and bubble coalescence phenomena of aqueous solutions of electrolytes. *Langmuir*, *11*(5), 1422–1426.

Xiao, Y., & Konermann, L. (2015). Protein structural dynamics at the gas/water interface examined by hydrogen exchange mass spectrometry. *Protein Science*, *24*(8), 1247–1256.

Yan, P., Jin, H., He, G., Guo, X., Ma, L., Yang, S., & Zhang, R. (2020). Numerical simulation of bubble

characteristics in bubble columns with different liquid viscosities and surface tensions using a cfd-pbm coupled model. *Chemical Engineering Research and Design*, *154*, 47–59.

Zahradnik, J., Peter, R., & Kastanek, F. (1987). The effect of liquid phase properties on gas holdup in bubble column reactors. *Collection of Czechoslovak Chemical Communications*, *52*(2), 335–347.

APPENDIX

APPENDIX I
ALL EXPERIMENTAL RESULTS

TABLE VII: The mass transfer coefficients, surface area, gas holdup and bubble size for each medium.

Medium	**k_La** (s^{-1})	**k_La** (h^{-1})	**A** (m^2)	**k_L** (m/s)	**gas holdup** $(-)$	**bubble diameter** (mm)	**a** (m^{-1})	**pH** $(-)$	**Ethanol concentration** $(g/L$
Water	0.0065	23.24	24.0	5.41E-07	9.20E-03	2.30	1.19E+04	7.0	0
Water, 5% ethanol	0.0420	151.09	192.3	4.43E-07	2.17E-02	0.68	9.47E+04		0
Mineral medium	0.0145	52.31	63.3	4.61E-07	1.39E-02	1.32	3.15E+04	6.3	0
Mineral medium, 5% ethanol	0.0235	84.66	179.9	2.65E-07	2.14E-02	0.71	8.88E+04	6.4	0
TUE C. autoethanogenum	0.0054	19.47	56.4	1.92E-07	1.36E-02	1.44	2.81E+04	5.6	0.7
TUE C. autoethanogenum, 5% ethanol	0.0191	68.78	257.9	1.50E-07	2.27E-02	0.53	1.27E+05	5.7	0.7
WUR R. rubrum	0.0042	14.95	70.4	1.18E-07	1.47E-02	1.25	3.51E+04	7.9	0
WUR R. rubrum, 5% ethanol	0.0092	33.18	442.4	4.22E-08	1.94E-02	0.26	2.19E+05	8.1	0
WUR C. autoethanogenum	0.0090	32.33	132.7	1.36E-07	1.70E-02	0.77	6.61E+04	5.0	0
WUR C. autoethanogenum, 5% ethanol	0.0074	26.65	204.5	7.34E-08	2.37E-02	0.70	1.01E+05	5.0	0
TUD C. autoethanogenum	0.0143	51.41	54.2	5.28E-07	1.25E-02	1.39	2.70E+04	5.9	Unknown
TUD C. autoethanogenum, 5% ethanol	0.0243	87.43	153.3	3.20E-07	2.02E-02	0.79	7.58E+04	5.9	Unknown

TABLE VIII: Overview of all experimental results

Medium	**Surface tension** $(mN/m)(37C)$	**Viscosity** (mPa/s)	**Density** $(kg/m^3)(37.0C)$	**Protein concentration** (μ/mL)	**Volume** (m^3)	**Dry weight empirical** (g_x/mL)	**Dry weight OD** (g_x/mL)
Water	69.02	0.768	992.91	0	2.01E-03	0	-
Water, 5% ethanol	52.20	0.827	984.36	0	2.03E-03	0	-
Mineral medium	68.62		996.28	0	2.01E-03	0	-
Mineral medium, 5% ethanol	51.49	0.825	986.63	0	2.03E-03	0	-
TUE C. autoethanogenum	68.82	0.732	997.62	1278.12	2.00E-03	0.246	0.207
TUE C. autoethanogenum, 5% ethanol	51.83	0.840	988.06	1278.12	2.02E-03	0.246	0.207
WUR R. rubrum	69.08	0.763	996.60	62.42	2.01E-03	0.504	-
WUR R. rubrum, 5% ethanol	51.76	0.759	987.93	62.42	2.02E-03	0.504	-
WUR C. autoethanogenum	69.54	0.778	995.75	563.38	2.01E-03	-	0.061
WUR C. autoethanogenum, 5% ethanol	52.69	0.833	986.92	563.38	2.03E-03	-	0.061
TUD C. autoethanogenum	70.43	0.821	997.97	369.13	2.00E-03	-	0.087
TUD C. autoethanogenum, 5% ethanol	51.66	0.815	989.28	369.13	2.02E-03	-	0.087

APPENDIX II
BUBBLE SIZE DISTRIBUTIONS IN DIFFERENT MEDIA

This appendix shows the bubble size distributions in the various media.

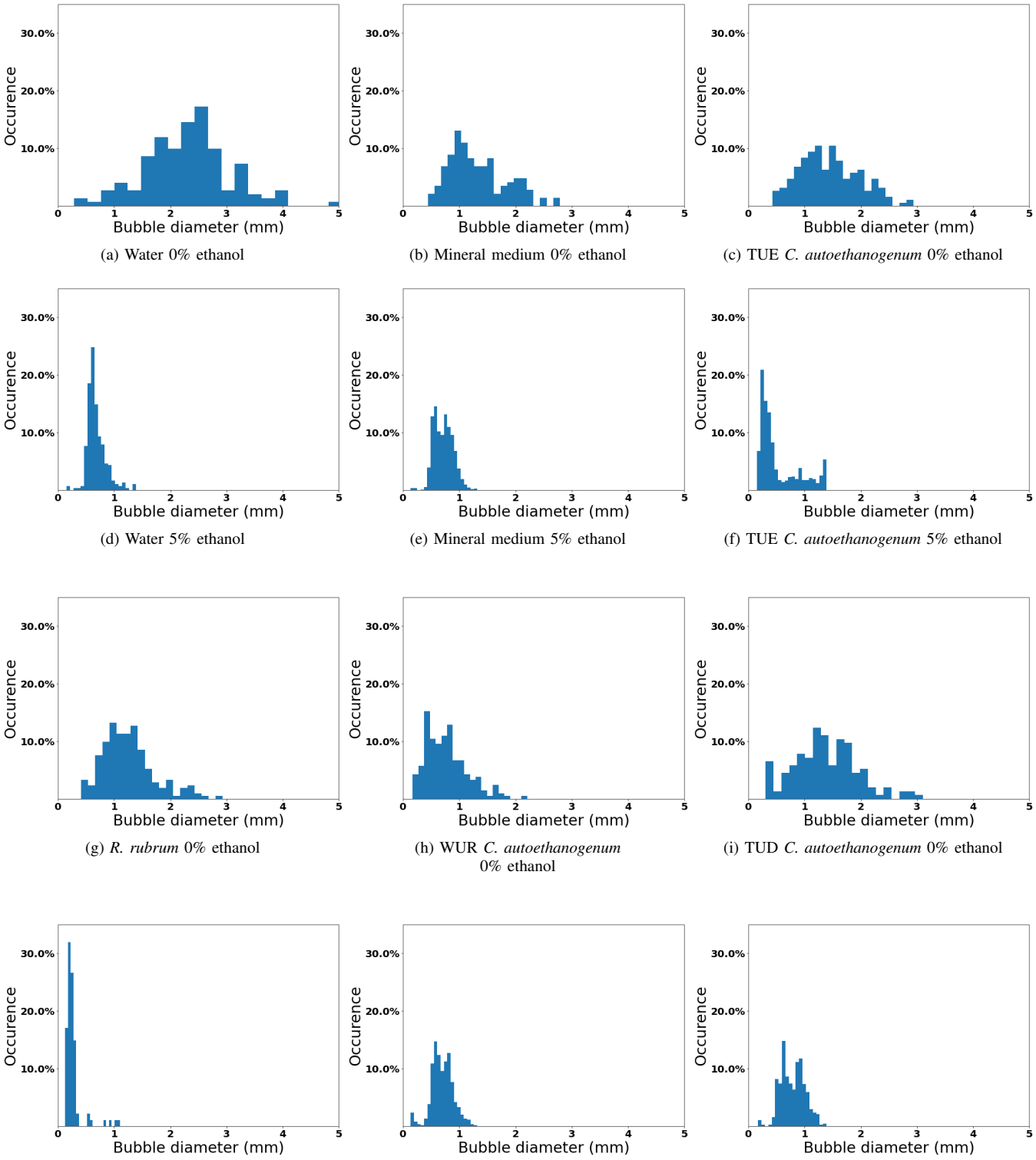

(a) Water 0% ethanol

(b) Mineral medium 0% ethanol

(c) TUE *C. autoethanogenum* 0% ethanol

(d) Water 5% ethanol

(e) Mineral medium 5% ethanol

(f) TUE *C. autoethanogenum* 5% ethanol

(g) *R. rubrum* 0% ethanol

(h) WUR *C. autoethanogenum* 0% ethanol

(i) TUD *C. autoethanogenum* 0% ethanol

(j) *R. rubrum* 5% ethanol

(k) WUR *C. autoethanogenum* 5% ethanol

(l) TUD *C. autoethanogenum* 5% ethanol

Fig. 15: Bubble size distribution of air in different media. At a superficial velocity of 0.191 m/s.

APPENDIX III
MICROSCOPE PICTURES OF THE FERMENTATION BROTHS

To determine the state of the cells in the used fermentation broths, the cells were analysed under a microscope with a 100X magnification. The cells in the broth with *C. autoethanogenum* from TUE all have a disrupted cell membrane. This shows that they are no longer alive. By the state of degradation of some of the cells it can be concluded that they have been dead for a while. The cells in the other broths are mostly still alive, seeing how they have a smooth cell membrane. In the broth with *C. autoethanogenum* from WUR, budding cells can be seen, which also indicates viable cells. The broth with *R. rubrum* from WUR has a contamination of smaller cells. It is not known which strain these cells are.

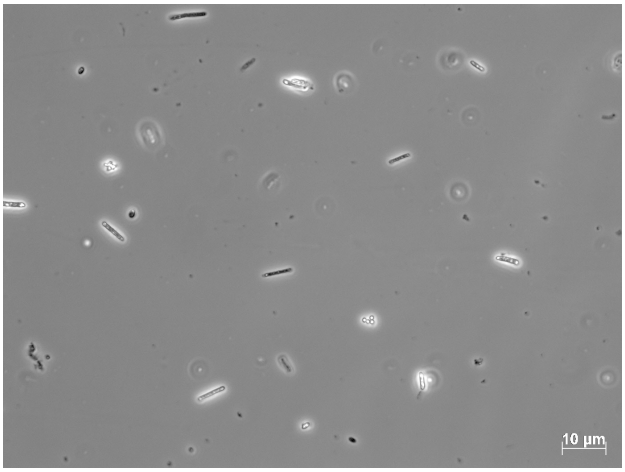

(a) *C. autoethanogenum*, TUE

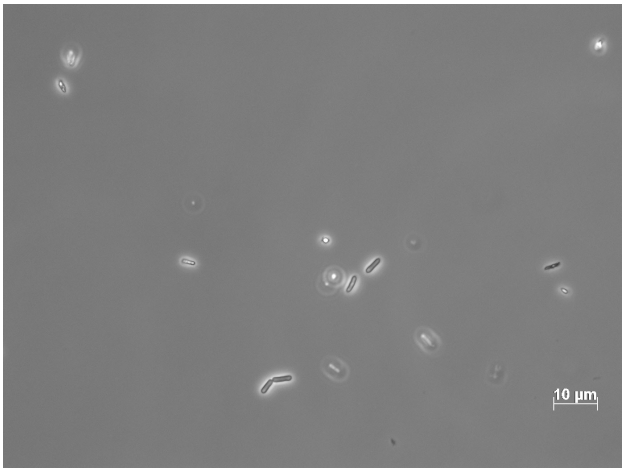

(b) *C. autoethanogenum*, WUR

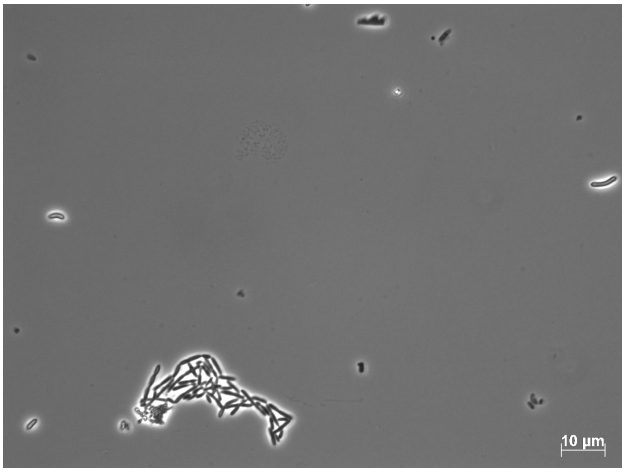

(c) *C. autoethanogenum*, TUD

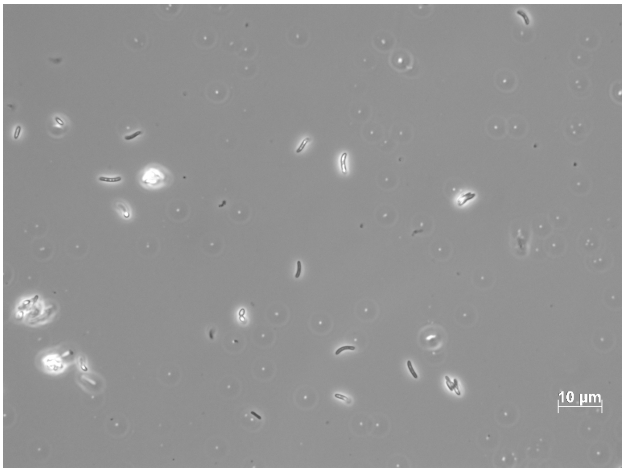

(d) *R. rubrum*, WUR

Fig. 16: The fermentation broths

APPENDIX IV
k_La MEASUREMENT IN BROTHS WITH OXYGEN CONSUMPTION

The k_La was also determined in a fermentation broth with *C. autoethanogenum*. However, because of the strong reducing agent in this medium, the oxygen concentration is not solely determined by the k_La but also by the oxygen consumption rate of the medium. To calculate the k_La of this medium, the oxygen consumption rate should be determined (Taguchi, 1966). The following method has been used for the determination of the k_La of the TUD broth with *C. autoethanogenum*. The oxygen consumption rate can be determined by turning the oxygen flow off when the medium is fully saturated with oxygen and measuring the decrease in the oxygen concentration. The rate at which this happens is equal to the oxygen consumption of the medium and can be calculated with:

$$\frac{dC_L}{dt} = -q_{O_2}\, C_x$$

When the oxygen consumption rate is known, the k_La can be determined using the following formula:

$$q_{O_2}\, C_x\, \Delta t + \Delta C_L = k_La \int_{t_1}^{t_2} (C^* - C_L)\, dt$$

With this method, it is assumed that the oxygen consumption is independent of the oxygen concentration of the medium.

The k_La could also have been determined by off-gas analysis in this case. But results with that method could not have been compared to results of the dynamic gassing out method, as different methods all have their own errors and thus can't be easily compared to each other (Suresh et al., 2009). Measuring the k_La of the other media with the off-gas analysis method is discouraged since a very sensitive off-gas analyser is needed to detect the small changes in the oxygen concentration that occur in small bioreactors (Garcia-Ochoa & Gomez, 2009).

After the column was incubated with the TUD and WUR *C. autoethanogenum* and cleaned thereafter. It was noticed that the DO probe did not return to 100% oxygen saturation in water. Since these probes work by means of reducing oxygen (Springer, 2009), the reducing agents that were present in these broths might have influenced the DO probe. No literature is found to understate this so this might be an interesting field for future research.

APPENDIX V
PYTHON SCRIPT FOR THE COMPUTATIONAL ANALYSIS OF THE BUBBLE DIAMETERS

The pictures that were taken with the SOPAT probe were analysed in Python using Houghs circle transformation (Huamán, n.d.). The Python script below gives a list with all bubble diameters, the mean bubble diameter and a bubble distribution plot as output. The SOPAT probe was set at a focal distance of 0.5 mm. According to the manual, at this distance a conversion factor from pixel to mm of $0.992555831 * 10^{-3}$ should be used. Figure 17 shows an example of circles that are drawn with the script. Only the bubbles that are in focus are counted because their size can be converted with the conversion factor.

```
#Importing modules
import numpy as np
import cv2 as cv
from matplotlib import pyplot as plt
from matplotlib.ticker import PercentFormatter


#Define function to detect circles
def circledetection(thisphoto):

    #Load image
    img = cv.imread(thisphoto)

    #Turn image to grayscale
    gray = cv.cvtColor(img, cv.COLOR_BGR2GRAY)
    gray = cv.medianBlur(gray, 5)


    #Detect circels, makes an array with 3 parameters, x, y and r
    circles = cv.HoughCircles(gray, cv.HOUGH_GRADIENT, 1. 400.
                              param1=100. param2=40. minRadius=60. maxRadius=700)

    #Ends function if no circles are found
    npcircles = np.array(circles)
    if npcircles.size == 1:
        return

    #For loop to extract the radius and turn into the diameter (in mm)
    for (x, y, r) in circles[0. :]:
        d = (2*r*0.992555831)/1000
        return d


#Set number of image and create diameters list
number_of_image = 1
diameters = []


while number_of_image <= 600: #adjust this value depending on the number of images in the f

    # Run circledetection function for each picture in the folder.
    # If no diameter is found, it is not added to the diameters array
    if number_of_image < 10:
        diameter = circledetection('folder/001_0000%d.bmp' % number_of_image)
        if diameter is not None:
            diameters.append(diameter)
        number_of_image += 1
    elif number_of_image > 9 and number_of_image < 100:
        diameter = circledetection('folder/001_000%d.bmp' % number_of_image)
```

```
        if diameter is not None:
            diameters.append(diameter)
        number_of_image += 1
    else:
        diameter = circledetection('folder/001_00%d.bmp' % number_of_image)
        if diameter is not None:
            diameters.append(diameter)
        number_of_image += 1



#Calculate the mean bubble diameter and the standard deviation
print("The mean diameter is:", np.mean(diameters), "mm")
print("The standard deviation is", np.std(diameters, ddof=(len(diameters)-1)))


# Create histogram
fig, axs = plt.subplots(1, 1, figsize=(10.7), tight_layout = True)
axs.hist(diameters, bins = 20. weights=np.ones(len(diameters)) / len(diameters))
plt.gca().yaxis.set_major_formatter(PercentFormatter(1))
plt.xlabel("Bubble diameter (mm)")
plt.ylabel("Occurence")
plt.show()
```

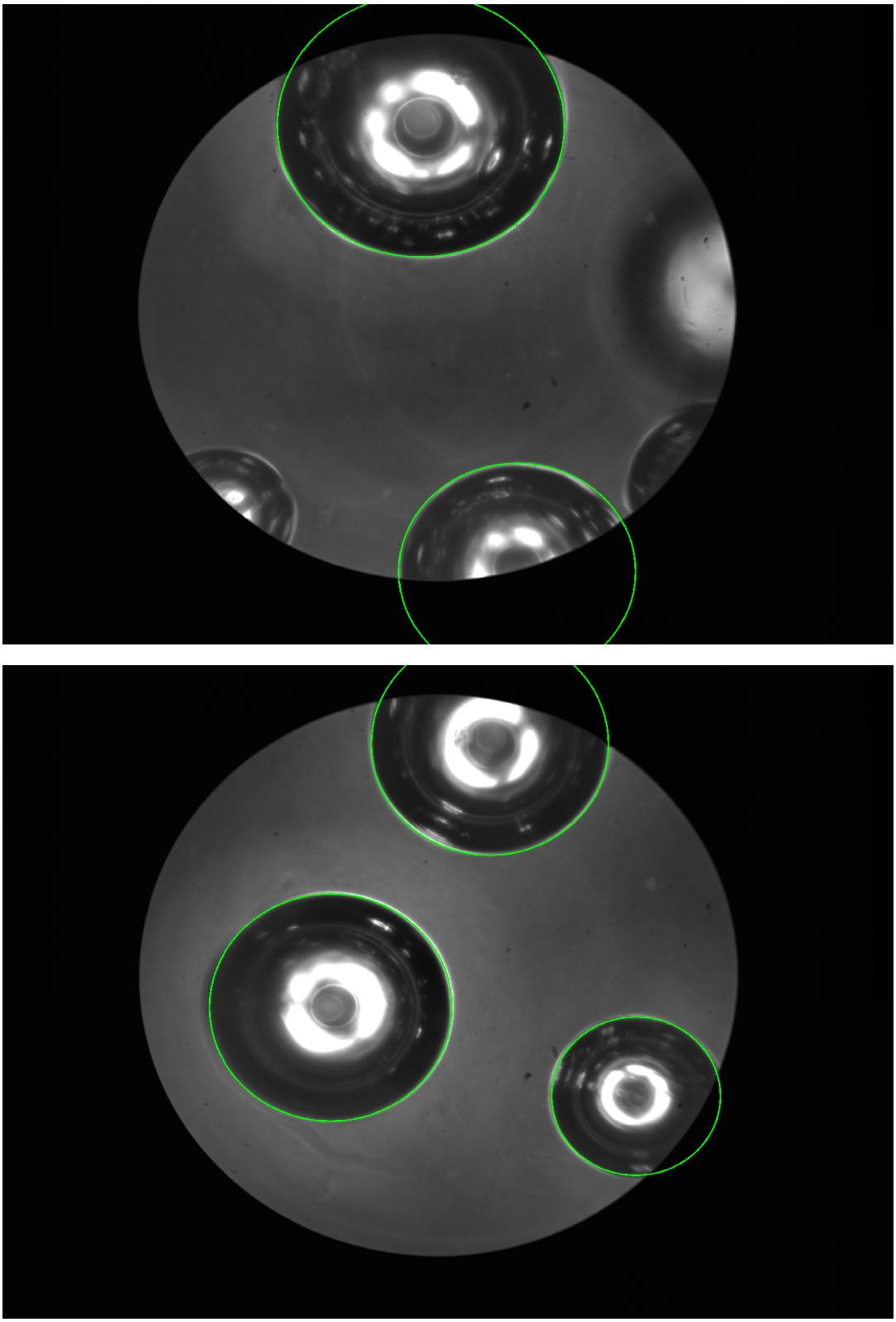

Fig. 17: Circles that are drawn with the script in the script above.

APPENDIX VI
BUBBLE RESIDENCE TIME

Because the surface tension is a dynamic parameter that is dependent on the bubble age, the bubble residence time in the bubble column needs to be determined. To achieve this, the bubble rise velocity is calculated with a formula as proposed by Park et al. (2017)(Dukhin et al., 1995):

$$v_b = \frac{1}{\sqrt{f_{sc}^2 \left(\frac{144\eta_L^2}{g^2 \rho_L^2 d_b^4} + \frac{\eta_L^{4/3}}{0.14425^2 g^{5/3} \rho_L^{4/3} d_b^3} \right) + \frac{1}{\frac{2.14\sigma_L}{\rho_L d_b} + 0.505 g d_b}}}$$

In this equation, the bubble diameter of spherical bubbles is used, which means that the Sauter bubble diameter will be used for non-spherical bubbles. f_sc is a factor which accounts for the suppressed internal gas circulation due to surface contaminants. This factor can be calculated with:

$$f_{sc} = 1 + \frac{0.5}{1 + exp\left(\frac{log(E_o+1)}{0.38}\right)}$$

E_o is the Eotvos number, a dimensionless number which indicates the ratio between body forces and surface tension forces. This can be calculated with:

$$E_o = \frac{g\rho_L d_b^2}{\sigma_L}$$

By multiplying the bubble rise velocity with the liquid height of the column, the bubble residence time can be calculated. With this residence time, the average surface tension can be determined. In the aforementioned equations the, the surface tension is used. This means, that the final surface tension and bubble velocity will be determined trough an iterative process.

These calculations are performed using the Python script below.

```
import math
import pandas as pd


#Define parameters
g = 9.81                            # gravitational constant, m/s^2
Hl = 0.6                            # liquid height, m


#Load excel
data = pd.read_excel('C:/Users/liloc/OneDrive/Documenten/BEP/Excel spul/Combi sheet.xlsx')

#define columns for parameters
media = data['Medium'].tolist()
mu_list = data['Viscosity (Pa/s)'].tolist()
rhoL_list = data['Density (kg/m3) (37.0C)'].tolist()
db_list = data['bubble diameter (mm)'].tolist()
sigmaL_list = data['Surface tension est. mN/m'].tolist()


# calculate bubble rise velocity for each medium
for medium, mu, rhoL, db, sigmaL in zip(media, mu_list, rhoL_list, db_list, sigmaL_list):
    print(medium)

    #adjust surface tension est.
    sigmaL = sigmaL / 1000

    #define Eo and fsc
    Eo = (g * rhoL * db**2)/sigmaL
    fsc = 1 + 0.5/(1 + math.exp(math.log10(Eo+1)/0.38))

    # calculate vb
    frac1 = 144 * mu**2 / (g**2 * rhoL**2 * db**4)
```

```
frac2 = mu**(4/3) / (0.14425**2 * g**(5/3) * rhoL**(4/3) * db**3)
subfrac3 = 2.14 * sigmaL / (rhoL * db)
frac3 = 1 / (subfrac3 + 0.505 * g * db)

vb = 1 / math.sqrt(fsc**2 * (frac1 + frac2) + frac3)

# Determine bubble residence time
t_br = Hl / vb

print("The bubble residence time is", t_br, "seconds")
```

APPENDIX VII
k_La EQUATIONS FROM LITERATURE

Several equations have been proposed to calculate the k_La, these correlations often use dimensionless numbers, as shown in Table IX Akita and Yoshida, 1973 Nakanoh and Yoshida, 1980 Kawase et al., 1987 Uchida et al., 1989 Vatai and Tekić, 1989

Equation	Name
$Sc = \frac{\eta_L}{\rho_L D_L}$	Schmidt
$Eo = \frac{\rho g D_r^2}{\sigma}$	Eötvos
$Ga = \frac{\rho^2 g D_r^3}{\eta_L^2}$	Galileo
$Fr = \frac{u_{s,g}}{g D_r}$	Froude
$Re = \frac{\rho u_{s,g} D_r}{\eta_L}$	Reynolds
$Sh = \frac{k_L D_r}{D_L}$	Sherwood

TABLE IX: Dimensionless numbers often used for k_La equations

In previous research the equations as shown in Table X are proposed. In the discussion, these are plotted against the measured k_La values of this experiment.

Source	Equation
Akita and Yoshida (1973)	$\frac{k_L a D^2}{D_L} = 0.6 \cdot \left(\frac{D^2 \rho g}{\sigma}\right)^{0.62} \cdot \left(\frac{D^3 \rho^2 g}{\mu^2}\right)^{0.3} \cdot \left(\frac{\mu}{\rho D_L}\right)^{0.5} \cdot \phi^{1.1}$
Nakanoh and Yoshida (1980)	$\frac{k_L a D^2}{D_L} = 0.09 \cdot \left(\frac{D^2 \rho g}{\sigma}\right)^{0.75} \cdot \left(\frac{D^3 \rho^2 g}{\mu^2}\right)^{0.4} \cdot \left(\frac{\mu}{\rho D_L}\right)^{0.5} \cdot \left(\frac{V_S}{\sqrt{gD}}\right)^{1}$
Kawase et al. (1987)	$\frac{k_L a D^2}{D_L} = 0.452 \cdot \left(\frac{D^2 \rho g}{\sigma}\right)^{0.6} \cdot \left(\frac{V_S}{gD}\right)^{0.3} \cdot \left(\frac{\mu}{\rho D_L}\right)^{0.5} \cdot \left(\frac{D V_S}{v_L}\right)$
Uchida et al. (1989)	$\frac{k_L a D^2}{D_L} = 0.17 \cdot \left(\frac{D^2 \rho g}{\sigma}\right)^{0.62} \cdot \left(\frac{D^3 \rho^2 g}{\mu^2}\right)^{0.3} \cdot \left(\frac{\mu}{\rho D_L}\right)^{0.5} \cdot \phi^{1.1}$
Vatai and Tekić (1989)	$\frac{k_L a D^2}{D_L} = 0.031 \cdot \left(\frac{D^2 \rho g}{\sigma}\right)^{0.75} \cdot \left(\frac{D^3 \rho^2 g}{\mu^2}\right)^{0.4} \cdot \left(\frac{\mu}{\rho D_L}\right)^{0.5} \cdot \left(\frac{V_S}{\sqrt{gD}}\right)^{1}$

TABLE X: Empirical correlations using dimensionless numbers to predict the k_La

The k_La values are calculated and visualised using the following Python script:

```
import pandas as pd
import matplotlib.pyplot as plt

#define parameters
dc = 0.0732          # bubble column diameter, m
g = 9.81             # gravitational constant, m2/s
ugs = 0.00182121313  # superficial gas velocity, m/s
Dl = 2 * 10**-9      # liquid diffusion coëfficient m2/s of oxygen in water
kl_w = 5.41 * 10**-7  # mass transfer coeff of water (m/s)


#Load data from combi sheet
data = pd.read_excel('C:/Users/liloc/OneDrive/Documenten/BEP/Excel spul/Combi sheet.xlsx',

#Load measured kla array
kla_m = data['kla (s-1)'].tolist()

#Load arrays per parameter
a_list = data['a (m-1)'].tolist()
kl_list = data['kl (m/s)'].tolist()
eg_list = data['gas holdup (-)'].tolist()
mu_list = data['viscosity (Pa/s)'].tolist()
rho_list = data['Density (kg/m3) (37.0C)'].tolist()
sigma_list = data['surface tension (N/m)'].tolist()

#create empty lists for equations kla's
```

```
Akita_Yoshida_list = []
Nakanoh_Yoshida_list = []
Kawase_list = []
Uchida_list = []
Vatai_Tekic_list = []

for a, kl, eg, mu, rho, sigma in zip(a_list, kl_list, eg_list, mu_list, rho_list, sigma_lis


    # Determine dimensionless numbers
    Sc = mu / (Dl * rho)     #schmidt number
    Eo = (g * rho * dc**2) / sigma #Eotvos number
    Ga = (g * dc**3 * rho**2) / mu**2 #Galileo number
    Fr = ugs / (g * dc)      #froude number
    Re = (rho * ugs * dc) / mu  #reynolds number


    #calculations for Sh * a * dc
    Akita_Yoshida_shadc = 0.6 * Eo**0.62 * Ga**0.3 * Sc**0.5 * eg**1.1
    Nakanoh_Yoshida_shadc = 0.09 * Eo**0.75 * Ga**0.4 * Sc**0.5 * Fr
    Kawase_shadc = 0.452 * Eo**0.62 * Ga**0.3 * Sc**0.5 * Fr * Re
    Uchida_shadc = 0.17 * Eo**0.62 * Ga**0.3 * Sc**0.5 * eg**1.1
    Vatai_Tekic_shadc = 0.031 * Eo**0.75 * Ga**0.4 * Sc**0.5 * Fr


    # transform to kla
    Akita_Yoshida = Akita_Yoshida_shadc * Dl / dc**2
    Nakanoh_Yoshida = Nakanoh_Yoshida_shadc * Dl / dc**2
    Kawase = Kawase_shadc * Dl / dc**2
    Uchida = Uchida_shadc * Dl / dc**2
    Vatai_Tekic = Vatai_Tekic_shadc * Dl / dc**2

    # append values to lists
    Akita_Yoshida_list.append(Akita_Yoshida)
    Nakanoh_Yoshida_list.append(Nakanoh_Yoshida)
    Kawase_list.append(Kawase)
    Uchida_list.append(Uchida)
    Vatai_Tekic_list.append(Vatai_Tekic)



plt.plot(kla_m, kla_m, label='Measured kla values')
plt.scatter(kla_m, Nakanoh_Yoshida_list, label="Nakanoh & Yoshida (1980)")
plt.scatter(kla_m, Kawase_list, label="Kawase et al. (1987)")
plt.scatter(kla_m, Uchida_list, label="Uchida et al. (1989)")
plt.scatter(kla_m, Vatai_Tekic_list, label="Vatai & Tekic (1989)")
plt.scatter(kla_m, Akita_Yoshida_list, label="Akita &Yoshida (1973)")
plt.xlabel('Measured kLa (s-1)')
plt.ylabel('Predicted kla (s-1)')
plt.legend()
plt.show()
```

STATISTICAL ANALYSIS

The significance of the results are evaluated with a Welch's t-test or a t-test based on Pearson's correlation coefficient.

Welch's t-test

To determine the significance of a difference between two samples, a Welch's t-test is used. This is a two sample, two sided t-test with unequal variances. The t statistic is calculated by:

$$\sigma = \sqrt{\frac{\sum (value_i - measuredmean)^2}{N-1}}$$

$$s = \sqrt{\frac{(N_1-1)\,\sigma_1^2 + (N_2-1)\,\sigma_2^2}{N_1+N_2-2} \cdot \left(\frac{1}{N_1}+\frac{1}{N_2}\right)}$$

$$tvalue = \frac{\bar{x}_1 - \bar{x}_2}{s}$$

Next, the p value is determined with the function "scipy.stats.sf(tvalue, degreesoffreedom) in Python and "T.DIST.2T(tvalue, degreesoffreedom)" in Microsoft Excel. When p<0.05. the difference is deemed as significant.

The k_La is calculated by determining the slope of a linear trendline. Because the reliability of the k_La is dependent on the fit of the slope, the weighted mean of the k_La values is used in this report and t-test. This is done by using the weighted mean in the t-test. This mean is calculated by:

$$weightedmean = \frac{\sum weight_i * value_i}{\sum weight_i}$$

The Python script that is used for these calculations can be found at the end of this Appendix.

Pearson correlation coefficient

To evaluate the significance of a linear correlation, the sample Pearson correlation coefficient is used. This coefficient can be calculated with:

$$r_{xy} = \frac{\sum x_i y_i - n\bar{x}\bar{y}}{\sqrt{\sum x_i^2 - n\bar{x}^2}\sqrt{\sum y_i^2 - n\bar{y}^2}}$$

With this value for r, the t-statistic can be calculated with:

$$t = r\sqrt{\frac{n-2}{1-r^2}}$$

With this t-statistic the p value can be determined with the aforementioned formula.

```
import scipy.stats as st
import numpy as np
import math

#This is a two sample, two sided welch's t-test.

# Make list with kla values and corresponding list with r^2 values
w0 = np.array([0.0063. 0.0064. 0.0067. 0.0064. 0.0065. 0.0067])
r_w0 = np.array([0.9959. 0.997. 0.9977. 0.9969. 0.9977. 0.8873])
w5 = np.array([0.0425. 0.041, 0.0415. 0.0387. 0.0457. 0.0505. 0.0416. 0.0475. 0.0419. 0.034
r_w5 = np.array([0.9794. 0.959. 0.9925. 0.9737. 0.9954. 0.9724. 0.9915. 0.9472. 0.9817. 0.9
f10 = np.array([0.0057. 0.0057. 0.0057. 0.0056. 0.0052. 0.0051. 0.0052. 0.005])
r_f10 = np.array([0.997. 0.997. 0.9983. 0.9956. 0.9922. 0.9915. 0.9947. 0.9901])
f15 = np.array([0.0185. 0.0212, 0.0191, 0.0174. 0.0204. 0.0181])
r_f15 = np.array([0.9953. 0.9934. 0.996. 0.9938. 0.9924. 0.9962])
fr0 = np.array([0.0043. 0.0059. 0.0064. 0.0066. 0.0062])
r_fr0 = np.array([0.9345. 0.986. 0.9947. 0.9966. 0.9958])
fr5 = np.array([0.0121, 0.0138. 0.0146. 0.0135])
r_fr5 = np.array([0.9723. 0.9857. 0.9922. 0.9864])
fw0 = np.array([0.0047. 0.0138. 0.0047])
r_fw0 = np.array([0.9405. 0.9717. 0.9197])
```

```
fw5 = np.array([0.0076. 0.0081, 0.0068. 0.0083])
r_fw5 = np.array([0.9302. 0.961, 0.9165. 0.9598])
mm0 = np.array([0.016. 0.0159. 0.0161])
r_mm0 = np.array([0.9882. 0.9919. 0.9918])
mm5 = np.array([0.025. 0.0254. 0.0262. 0.0269])
r_mm5 = np.array([0.9856. 0.9814. 0.9888. 0.9898])
fd0 = np.array([0.01358094. 0.015912307. 0.013472096. 0.014154815])
r_fd0 = np.array([0.98. 0.98. 0.98. 0.98])
fd5 = np.array([0.024137786. 0.023589305. 0.025121633. 0.024290822])
r_fd5 = np.array([0.98. 0.98. 0.98. 0.98])

# relate fr to the kla of water that morning by dividing assumed kla of water by water kla
conversionfactor_fr = 0.009215321723667378 / 0.0098
fr0 = np.multiply(fr0. conversionfactor_fr)
fr5 = np.multiply(fr5. conversionfactor_fr)
conversionfactor_fw = 0.009215321723667378 / 0.0099
fw0 = np.multiply(fw0. conversionfactor_fw)
fw5 = np.multiply(fw5. conversionfactor_fw)
conversionfactor_mm = 0.0089 / 0.0098
mm0 = np.multiply(mm0. conversionfactor_mm)
mm5 = np.multiply(mm5. conversionfactor_mm)


#Make array's with and without ethanol
noeth = np.append(w0. f10)
noeth = np.append(noeth, fr0)
noeth = np.append(noeth, fd0)
noeth = np.append(noeth, mm0)
eth = np.append(w5. f15)
eth = np.append(eth, fr5)
eth = np.append(eth, fd5)
eth = np.append(eth, mm5)
r_noeth = np.append(r_w0. r_f10)
r_noeth = np.append(r_noeth, r_fr0)
r_noeth = np.append(r_noeth, r_fd0)
r_noeth = np.append(r_noeth, r_mm0)
r_eth = np.append(r_w5. r_f15)
r_eth = np.append(r_eth, r_fr5)
r_eth = np.append(r_eth, r_fd5)
r_eth = np.append(r_eth, r_mm5)

# define function for weighted, welch's t-tests, returns the t-statistic and p-value
def ttest(x, y, wx, wy):
    #substract 0.9 from weight arrays to get to the weight
    wx = wx - 0.9
    wy = wy - 0.9

    # Calculate weighted mean
    meanx = np.sum(np.multiply(x, wx)) / np.sum(wx)
    meany = np.sum(np.multiply(y, wy)) / np.sum(wy)

    # Fill array to calculate the standard deviation
    sigma_array_x = []
    sigma_array_y = []

    for i in x:
        i_sigma = (i - meanx)**2
```

```
        sigma_array_x.append(i_sigma)

    for j in y:
        j_sigma = (j - meany)**2
        sigma_array_y.append(j_sigma)

    sd_x = math.sqrt(np.sum(sigma_array_x) / (len(x)-1))
    sd_y = math.sqrt(np.sum(sigma_array_y) / (len(y)-1))

    # Perform two sample, two sided welch's t-test
    s = math.sqrt((len(x)-1)*sd_x**2 + (len(y)-1)*sd_y**2 * (1/len(x)+1/len(y)) / (len(x)+l
    t = (meanx-meany)/s
    p = st.t.sf(abs(t), df=(len(x)+len(y)-2)) * 2

    # Print important values
    print("t value:", t)
    print("p value:", p)
    print("meanx", meanx)
    print("meany", meany)


print('t-test: without ethanol, with ethanol')
ttest(noeth, eth, r_noeth, r_eth)
```

APPENDIX VIII
DRY WEIGHT DETERMINATION

The determination of the biomass concentration consisted of the following steps [2]:

1. Pre-ash aluminum cups in an oven at 500 °C.
2. Measure the weight of each cup and put aside in a dry place.
3. Fill three tubes with 50 mL of the sample each. Measure the weight of the tubes, they should not diverge more than 3 grams in weight.
4. Centrifuge the tubes thoroughly.
5. Discard the supernatant.
6. Resuspend the pellets in MilliQ-water and pour each solution in one of the aluminum cups.
7. Leave overnight in an oven of 105 °C.
8. Put the cups in an oven of 550 °C.
9. Weigh each cup, and subtract the weight of the empty cup from this. Add the values of the three cups for the amount of biomass in 150 mL of medium.

[2]This is a simplification of the real protocol.

PREPARATIONS OF MINERAL MEDIA

The mineral media that were used in the fermentors to prepare the fermentation broths are prepared as follows:

Mineral medium from TUD C. autoethanogenum

This is also the mineral medium that is used in the experiments without biomass.

The protocols for the ”Vitamin solution WUR 500x”, ”Trace Elements SL-10” and ”Trace Elements Alkaline 5000x” of the TUD medium are listed below.

Experiment: Preparation of Feed Medium **Preparation Date:**
Experiment code/label:
Project: Process Integrated Syngas Conversion Technology **Project Code:** TBMC53

Preparation of Feed Medium (for *C. autoethanogenum*)

- Prepare the total amount of medium. Volume: 4 L

Compound	Formula	CAS no/ Location	Desired concentration per liter	Amount to be weigh/add		Amount weighed / added
Ammonium chloride	NH_4Cl	12125-02-9	0.90 g/L	3.6	g	
Sodium chloride	NaCl	7647-14-5	0.90 g/L	3.6	g	
Magnesium sulfate heptahydrate	$MgSO_4 \times 7\ H_2O$	10034-99-8	0.20 g/L	0.8	g	
Monopotassium phosphate	KH_2PO_4	7778-77-0	0.75 g/L	3	g	
Dipotassium phosphate	K_2HPO_4	7758-11-4	1.5 g/L	6	g	
Calcium chloride dihydrate	$CaCl_2 \times 2\ H_2O$	10035-04-8	0.02 g/L	0.08	g	
Na-resazurin stock solution (0.5 g/L)	$C_{12}H_6NNaO_4$	62758-13-8	1.00 mL/L	4	mL	
Trace element Acid (1000x)	Trace element solution Acid	-	1.0 mL/L	4	mL	
Trace element Basic (5000x)	Trace element Basic	-	0.2 mL/L	0.8	ml	
Bacto Yeast Extract			0.5 g/L	2	g	
Vitamin solution WUR** (500x)	Vitamin solution WUR	-	2 mL/L	4	mL	
L-Cysteine hydrochloride monohydrate *	L-Cysteine-HCl x H2O (50 g/L)	52-89-1	Stock: 15 mL/L (Final: 0.75 g/L)	30	mL	

- Dissolve ingredients (except sterile additions) in demi H_2O and fill volume to 4 L.

Experiment: Preparation of Stock Solution of Vitamins **Preparation Date:** Dec , 2020
Experiment code/label: 201907-PREP-03
Project: Process Integrated Syngas Conversion Technology **Project Code:** TBMC53

Preparation of Stock Solution of Vitamins WUR 500x

- Prepare the total amount of medium. Volume: 1000 mL

Compound	Formula	CAS no/ Location	Desired concentration per liter	Amount to be weigh (g)	Amount weighed (g)
Biotin (vitamin B_7)	$C_{10}H_{16}N_2O_3S$	Fridge MSD kitchen	10 mg	0.0100 g	
Nicotinamide (vitamin B_3)	$C_6H_6N_2O$	B0.620/R5/S2	100 mg	0.1000 g	
p-aminobenzoic acid	$H_2NC_6H_4CO_2H$	B0.620/R5/S2	50 mg	0.0500 g	
Thiamine hydrochloride (vitamin B_1)	$C_{12}H_{17}ClN_4OS \cdot HCl$	B0.620/C2/S1	100 mg	0.1000 g	
Pantothenic acid hemicalcium salt (vitamin B_5)	$HOCH_2C(CH_3)_2CH(OH)CONHCH_2CH_2CO_2 \cdot 1/2Ca$	B0.620/R5/S2	50 mg	0.0500 g	
Pyridoxamine	$C_8H_{12}N_2O_2 \cdot 2HCl$	B0.620/F5	250 mg	0.2500 g	
Cyanocobalamine (vitamin B_{12})	$C_{63}H_{88}CoN_{14}O_{14}P$	B0.620/R5/S2	50 mg	0.0500 g	
Riboflavin (vitamin B_2)	$C_{17}H_{20}N_4O_6$	B0.620/C2/S1	50 mg	0.0500 g	

Final weight solution: _____

- Dissolve the vitamins in demi water
- Fill with demi water up to final volume
- Measure final pH of solution:
- Label the bottle (with code of experiment): 201907-PREP-03
- Store solution in fridge (+ 4°C). Wrap bottle in Aluminium (consider filter sterilization)

Experiment: Preparation of Stock Solution of Trace Elements SL-10 **Preparation Date:** July , 2019
Experiment code/label: 201907-PREP-01
Project: Process Integrated Syngas Conversion Technology **Project Code:** TBMC53

Preparation of Stock Solution of Trace Elements SL-10 (ACID)

- Prepare the total amount of medium. Volume: 500 mL

Compound	Formula	CAS no/ Location	Desired concentration per liter	Amount to be weigh (g)	Amount weighed (g)
Hydrochloric acid	HCl (25%; 7.7 M)	7647-01-0	10.00 ml	5 mL	
Iron(II) chloride tetrahydrate	$FeCl_2$ x 4 H_2O	13478-10-9	1.50 g	0.7500 g	
Iron(III) chloride hexahydrate	$FeCl_3$·6 H_2O	10025-77-1	2.50 g	1.2500 g	
Zinc chloride	$ZnCl_2$	7646-85-7	70.00 mg	0.0350 g	
Manganese(II) chloride tetrahydrate	$MnCl_2$ x 4 H_2O	13446-34-9	100.00 mg	0.0500 g	
Boric acid	H_3BO_3	10043-35-3	6.00 mg	0.0030 g	
Cobalt(II) chloride hexahydrate	$CoCl_2$ x 6 H_2O	7791-13-1	190.00 mg	0.0950 g	
Copper(II) chloride dihydrate	$CuCl_2$ x 2 H_2O	10125-13-0	2.00 mg	0.0010 g	
Nickel(II) chloride hexahydrate	$NiCl_2$ x 6 H_2O	7791-20-0	24.00 mg	0.0120 g	
Sodium molybdate dihydrate	Na_2MoO_4 x 2 H_2O	10102-40-6	36.00 mg	0.0180 g	

Final weight solution: _____

- Dissolve the salt $FeCl_2$ in HCL solution
- Dissolve, then, the salt $FeCl_3$ in the same solution
- Dilute with demi water, add and dissolve the other salts
- Fill with demi water up to final volume
- Measure final pH of solution:
- Label the bottle (with code of experiment): 201907-PREP-01
- Store solution in fridge (+ 4°C). Wrap bottle in Aluminium (consider filter sterilization)

Experiment: Preparation of Stock Solution of Trace Elements Basic **Preparation Date:** July , 2019
Experiment code/label: 201907-PREP-02
Project: Process Integrated Syngas Conversion Technology **Project Code:** TBMC53

Preparation of Stock Solution of Trace Elements Alkaline 5000x

- Prepare the total amount of medium. Volume: 250 mL

Compound	Formula	CAS no/ Location	Desired concentration per liter	Amount to be weigh (g)	Amount weighed (g)
Sodium Hydroxide	NaOH	1310-73-2	400 mg	0.1000 g	
Sodium selenite	Na2SeO3	10102-18-8	17.29 mg	0.0043 g	
Sodium tungstate dihydrate	Na2WO4.2H2O	10213-10-2	1032.98 mg	0.2582 g	
Sodium molybdate dihydrate	Na2MoO4.2H2O	10102-40-6	24.195 mg	0.0060 g	

Final weight solution: _____

- Dissolve the NaOH pellets in water
- Dissolve, then, the salt remaining salts in the basic solution
- Fill with demi water up to final volume
- Measure final pH of solution:
- Label the bottle (with code of experiment): 201907-PREP-02
- Store solution in fridge (+ 4°C). Wrap bottle in Aluminium (consider filter sterilization)

Mineral medium from WUR and TUE

The fermentation broths from WUR and TUE are grown on the same mineral medium, which is listed below. For the fermentation broths with *C. autoethanogenum* 1 g/L Yeast extract is added.

4
+CPMedia-1-

Stock solutions to be used to "compose" all the media:
All concentrations are given in grams per litre.

Solution 1: 27.2 g KH_2PO_4

Solution 2: 35.6 g $Na_2HPO_4.2H_2O$

Solution 3A: 24 g NH_4Cl; 24 g NaCl; 8 g $MgCl_2.6H_2O$

Solution 3B: 11 g $CaCl_2.2H_2O$

Solution 4: 80 g $NaHCO_3$

Trace elements: Acid Stock Solution (I)

50 mM HCl	1.8 g
1 mM H_3BO_3	61.8 mg
0.5 mM $MnCl_2$	61.25 mg
7.5 mM $FeCl_2$	943.5 mg
0.5 mM $CoCl_2$	64.5 mg
0.1 mM $NiCl_2$	12.86 mg
0.5 mM $ZnCl_2$	67.7 mg
0.1 mM $CuCl_2$	13.35 mg

Alkaline Stock solution (II)

10 mM NaOH	400 mg
0.1 mM Na_2SeO_3	17.3 mg
0.1 mM Na_2WO_4	29.4 mg
0.1 mM Na_2MoO_4	20.5 mg

(Or any other trace metal mixture.)

Vitamins:

Biotin	20 mg
Nicotinamid	200 mg
p-Aminobenzoic acid	100 mg
Thiamin (Vit B1)	200 mg
Panthotenic acid	100 mg
Pyridoxamine	500 mg
Cyanocobalamine (Vit B12)	100 mg
Riboflavine	100 mg

(Or any other vitamin mixture.)

Solution 7: 240.2 g $Na_2S.9\ H_2O$ Store under N_2 and in the dark
Na_2S is not stable in water due to chemical reactions. Make a fresh stock every month

Solution 8: 0.5 g Resazurin

CPMedia-2-

PREPARATION OF REDUCED MEDIA FOR THE CULTIVATION OF ANAEROBES.

Composition per liter medium.

MINERAL SALTS MEDIUM, bicarbonate buffered (Code: **BM**)

Add before autoclaving (use an erlenmeyer):
500 ml dH_2O
1 ml solution 8
15 ml solution 1
15 ml solution 2
12.5 ml solution 3A
1 ml solution trace I
1 ml solution trace II

-1% v/v of a filter sterilised calcium/vitamin-solution; make up per litre medium:
10 ml sol 3B + 1 ml vitamin solution.
(so: in 50 ml medium you add 0.5 ml of the sterilized Ca/Vit mixture)

-Add the carbon source.

-Add 2% Yeast extract solution 50g/L
-Add 2% Tryptone solution 50 g/L

Finally, to completely reduce the medium add:
- 5% v/v of a sterilized reducing solution; make up per litre medium:
50 ml sol.4 + 1 ml sol.7 + 0.5 gram cystein
(so: in 50 ml medium you add 2.5 ml of the bicarb/sulf/cyst mixture)

CPMedia-3-

Other possible vitamins and trace element mixture::

Vitamin mixture;
2 mg Biotin; 2 mg Folic acid; 10 mg Vit. B6 (pyrodoxine HCl); 5 mg Vit B2 (Riboflavine); 5 mg Vit B1 (Thiamine HCl); 5 mg Nicotinamide; 5 mg Vit B12 (Cyanocobalamin); 5 mg p-Aminobenzoic acid; 5 mg Lipoic acid (Thioctic acid); 5 mg Pantothenic acid.

ADD 1-10 ML TO A MINERAL SALTS MEDIUM.

Trace elements;
2 g $FeCl_2.4H_2O$; 0.05 g H_3BO_3; 0.05 g $ZnCl_2$; 0.03 g $CuCl_2$; 0.05 g $MnCl_2.4H_2O$; 0.05 g $(NH_4)_6Mo_7O_{24}.4H_2O$; 0.05 g $AlCl_3$; 0.05 g $CoCl_2.6H_2O$; 0.05 g $NiCl_2$; 0.5 g EDTA; 1 ml. conc. HCl.

In general: if compounds are heat stable; add before autoclaving; if the compounds are not heat stable or react in any way with either the medium components or the rubber stopper: filter sterilize and add after autoclaving.